Morphometric analysis of Skiagia-plexus acritarchs from the early Cambrian of North Greenland: toward a meaningful evaluation of phenotypic plasticity

Authors: Wallet, Elise, Willman, Sebastian, and Slater, Ben J.

Source: Paleobiology, 48(4) : 576-600

Published By: The Paleontological Society

URL: https://doi.org/10.1017/pab.2022.12

Paleobiology, 48(4), 2022, pp. 576–600
DOI: 10.1017/pab.2022.12

PALEOBIOLOGY
A PUBLICATION OF THE Paleontological SOCIETY

Article

Morphometric analysis of *Skiagia*-plexus acritarchs from the early Cambrian of North Greenland: toward a meaningful evaluation of phenotypic plasticity

*Elise Wallet**, *Sebastian Willman*, *and Ben J. Slater*

Abstract.—The Cambrian evolutionary radiations are marked by spectacular biotic turnovers and the establishment of increasingly tiered food chains. At the base of these food chains are primary producers, which in the Cambrian fossil record are chiefly represented among organic-walled microfossils. The majority of these microfossil remains have traditionally been attributed to an informal category of incertae sedis called "acritarchs," based entirely on form taxonomy. Acritarch form taxa have been intensely used for biostratigraphy and in large-scale studies of phytoplankton diversity. However, both prospects have been challenged by cases of taxonomic inconsistencies and oversplitting arising from the large phenotypic plasticity seen among these microfossils. The acritarch form genus *Skiagia* stands as an ideal case study to explore these taxonomic challenges, because it encompasses a number of form species widely used in lower Cambrian biostratigraphy. Moreover, subtle morphological differences among *Skiagia* species were suggested to underlie key evolutionary innovations toward complex reproductive strategies. Here we apply a multivariate morphometric approach to investigate the morphological variation of *Skiagia*-plexus acritarchs using an assemblage sourced from the Buen Formation (Cambrian Series 2, Stages 3–4) of North Greenland. Our analysis showed that the species-level classification of *Skiagia* discretizes a continuous spectrum of morphologies. While these findings bring important taxonomic and biostratigraphic hurdles to light, the unequal frequency distribution of life cycle stages among *Skiagia* species suggests that certain elements of phytoplankton paleobiology are nonetheless captured by *Skiagia* form taxonomy. These results demonstrate the value of using morphometric tools to explore acritarch phenotypic plasticity and its potential ontogenetic and paleoecological drivers in Cambrian ecosystems.

Elise Wallet, Sebastian Willman, and Ben J. Slater. Palaeobiology Programme, Department of Earth Sciences, Uppsala University, Villavägen 16, SE-75236 Uppsala, Sweden. E-mail: elise.wallet@geo.uu.se, sebastian.willman@geo.uu.se, ben.slater@geo.uu.se

Accepted: 18 March 2022
*Corresponding author.

Introduction

Throughout the Proterozoic and early Paleozoic records, most organic-walled microfossils consist of vesicular remains of uncertain biological affinity, collectively assigned to the informal group "Acritarcha" (Evitt 1963). Acritarchs have traditionally been classified using an essentially phenetic form-taxonomic scheme (Downie et al. 1963; Evitt 1963) routinely used in biostratigraphy. In particular, the abundance and cosmopolitan distribution of many acritarch taxa throughout the Cambrian Period (Molyneux et al. 2013) have led to the extensive use of acritarchs to correlate regional biostratigraphic schemes previously based on skeletal faunas or to provide relative age constraints in areas where other sources are absent (Moczydłowska 1991, 1998, 1999; Moczydłowska and Zang 2006; Zang et al. 2007; Palacios et al. 2011, 2018, 2020; Rushton et al. 2011; Ahn and Zhu 2017).

Despite being evidently polyphyletic, morphological and ultrastructural evidence suggests that a substantial subset of Cambrian acritarchs represent various developmental stages in the life cycle of unicellular phytoplankton (Tappan 1980; Colbath and Grenfell 1995; Talyzina and Moczydłowska 2000; Moczydłowska 2010, 2016). These comprise the

0094-8373/22

numerous small (<100 μm), symmetrical acanthomorphs (process-bearing acritarchs) often preserving excystment structures (Butterfield 1997; Talyzina and Moczydłowska 2000; Knoll et al. 2006; Moczydłowska and Willman 2009; Moczydłowska 2010). As such, the acritarch record offers crucial, albeit indirect, glimpses into the evolution of primary producers from a time when complex multi-tiered food webs were first being established during the Cambrian (Butterfield 1997, 2007, 2011; Vidal and Moczydłowska-Vidal 1997; Moczydłowska 2002, 2011; Peterson and Butterfield 2005).

Large-scale patterns of phytoplankton diversity have traditionally been explored using form-taxonomic counts (Tappan and Loeblich 1973; Vidal and Knoll 1982; Knoll 1994; Strother 1996, 2008; Vidal and Moczydłowska-Vidal 1997; Moczydłowska 1998, 2011; Knoll et al. 2006; Nowak et al. 2015; Zheng et al. 2020) and compared with corresponding metazoan diversity (Moczydłowska 2002, 2011; Butterfield 2004; Nowak et al. 2015). A meaningful evaluation of the timing and patterns of early phytoplankton evolution has nevertheless been hampered by problems of form taxonomy and the polyphyletic nature of acritarchs. As well as concealing diversity sourced from multiple distantly related clades, a direct diversity-based reading of the acritarch record is further confounded by the problems of distinguishing ecophenotypic or ontogenetic variants. Indeed, modern algal protists exhibit tremendous intraspecific disparity, expressed as successive growth stages dependent on a variety of environmental parameters (e.g., Sandgren 1983; Kokinos and Anderson 1995; Ellegaard 2000; Luo et al. 2005; Naselli-Flores et al. 2007). When imparted to the fossil record, such phenotypic plasticity could act to artificially inflate "species" diversity, or conversely deflate diversity through instances of morphological convergence. For instance, morphologically simple form taxa such as *Leiosphaeridia* are almost certainly produced by a wide range of more or less distantly related clades (Butterfield et al. 1994; Talyzina and Moczydłowska 2000; Willman and Moczydłowska 2007; Javaux and Knoll 2017; Slater and Budd 2019), leading to an underestimation of phytoplankton diversity (and/or the inclusion of non-phytoplankton). By contrast, individual biological species may produce a spectrum of cysts, envelopes, and other recalcitrant structures throughout their life cycles, each of which may have been described as a distinct acritarch taxon, resulting in an overestimation of standing diversity (Butterfield 2004, 2005a,b). Postmortem chemical and physical processes add another problematic dimension to a direct reading of acritarch diversity, because such processes can result in a range of secondary features that are easily mistaken for diagnostic ones (e.g., split or curled processes; Grey and Willman 2009). Difficulties in recognizing form taxa beyond underlying sources of taphonomic, ontogenetic, and/or other intraspecific variation has led to significant inconsistencies in naming (Stricanne and Servais 2002; Servais et al. 2004; Mullins and Servais 2008).

The range of small acanthomorphic acritarchs encompassed by the Cambrian form genus *Skiagia* typifies these taxonomic dilemmas. The morphology and dimensions of the diagnostically funnel-shaped processes of *Skiagia* form the basis of its species-level subdivisions (Downie 1982; Moczydłowska 1991, 1998). These subtle differences in the specific taxonomy of *Skiagia* have been used to correlate uppermost Fortunian to basal Miaolingian sedimentary successions worldwide (Moczydłowska 1991, 1999; Moczydłowska and Zang 2006; Landing et al. 2013). In particular, two widely used markers are the first appearance datum (FAD) of *Skiagia ornata*, which slightly precedes the as yet undefined Fortunian/Cambrian Stage 2 boundary; and the FAD of *Skiagia ciliosa*, which lies within Cambrian Stage 3, below the first appearance of olenellid trilobites. More recently, however, species of the *Skiagia*-plexus have been recognized as distinct stages in an algal life cycle (Moczydłowska 2010), a factor at odds with their sequential appearance in the fossil record (Zhang et al. 2017; Palacios et al. 2020). As with many acritarch form taxa, *Skiagia* species are also characterized by extended synonymy lists and ambiguous transitional morphotypes (Moczydłowska 1991, 2011) detailing a history of taxonomic

inconsistencies. A critical evaluation of the taxonomy of this important acritarch is therefore needed.

Here we take a novel approach to this persistent problem and use multivariate ordination techniques to shed light on the morphological matrix underlying the definition of *Skiagia* species and their phenotypic variation, following the principles of population analysis (Le Hérissé 1989; Fatka and Brocke 2008). Palynological preparations from a previous study (Vidal and Peel 1993) were used to detect morphological patterns of variation in *Skiagia* at the scale of a single siliciclastic succession from the Buen Formation (Cambrian Series 2, Stages 3–4), North Greenland. Combined with an independent examination of life cycle stages and their discrete features, this quantitative approach offers the prospect of clarifying the complex relationships among morphology, taxonomy, and paleobiology in a local *Skiagia* population.

Materials and Methods

Sampled Locality and Stratigraphy

This study is based on acritarch assemblages from two horizons in the lower Cambrian Buen Formation at the Brillesø site, southern Peary Land, North Greenland (Fig. 1). The geological and biostratigraphic context of the sampled locality is outlined below.

The Buen Formation (Cambrian Stages 3–4) mainly outcrops along an east-west-trending belt extending eastward to the southern margin of Peary Land (Fig. 1A,B). Successions from these localities are informally subdivided into a sandstone-dominated lower member deposited in shallow-shelf settings and a mudstone-dominated upper member deposited in outer-shelf conditions (Vidal and Peel 1993; Ineson and Peel 1997; Fig. 1C). A more detailed account of the early Cambrian geology of North Greenland is given by Higgins et al. (1991), Vidal and Peel (1993), Ineson and Peel (1997, 2011), and Peel and Willman (2018).

The Brillesø site (southern Peary Land; Fig. 1A) previously yielded both acritarchs (Vidal and Peel 1993) and small carbonaceous fossils (Slater et al. 2018; Wallet et al. 2021) from the upper member of the Buen Formation. The acritarch assemblage has previously been assigned to the *Heliosphaeridium dissimilare–Skiagia ciliosa* Zone of Dyeran Stage (Cambrian Stages 3–4; Vidal and Peel 1993; Fig. 2). It includes *Skiagia ciliosa*, *Skiagia* cf. *pura*, *Pterospermella solida*, *Cymatiosphaera* cf. *postii*, *Leiovalia tenera*, *Multiplicisphaeridium dendroideum*, *Heliosphaeridium dissimilare*, *Heliosphaeridium lubomlense*, *Heliosphaeridium obscurum*, and *Goniosphaeridium* cf. *volkovae*. Reexamination of the palynological material retrieved by Vidal and Peel (1993) also revealed the presence of *Pterospermella velata* (Fig. 2I) and

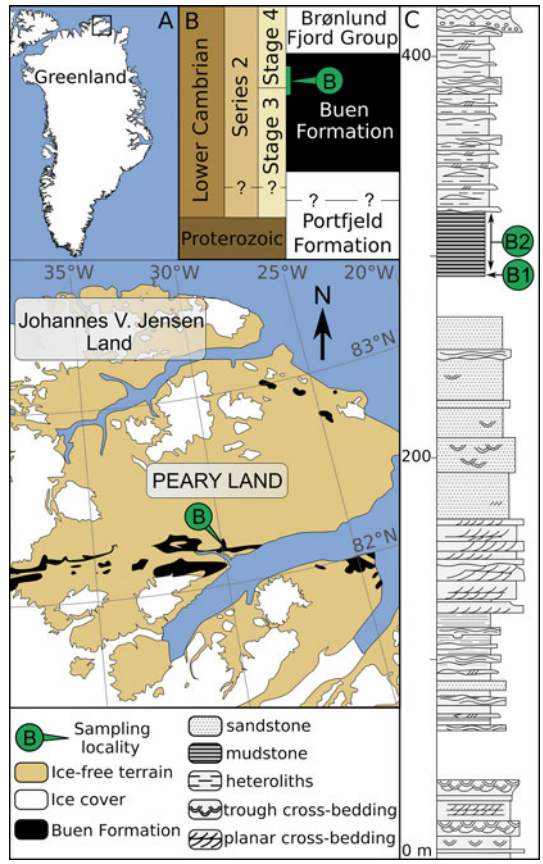

FIGURE 1. Geological map and stratigraphy of the sampled area (redrawn from Wallet et al. 2021). A, Map of Greenland with magnified area showing the lateral extent of early Cambrian strata in southern Peary Land (after Soper and Higgins 1987). B, Stratigraphic subdivision of Neoproterozoic–early Cambrian sediments in North Greenland and their tentative correlation with the international stratigraphic chart (after Ineson and Peel 2011). Inferred stratigraphic location of sampled horizons is shown in green. C, Sedimentary log of the Buen Formation at its type locality and nearby outcrops (after Vidal and Peel 1993), showing sampled horizons at Brillesø locality 1 (B1) and Brillesø locality 2 (B2; Peel and Willman 2018).

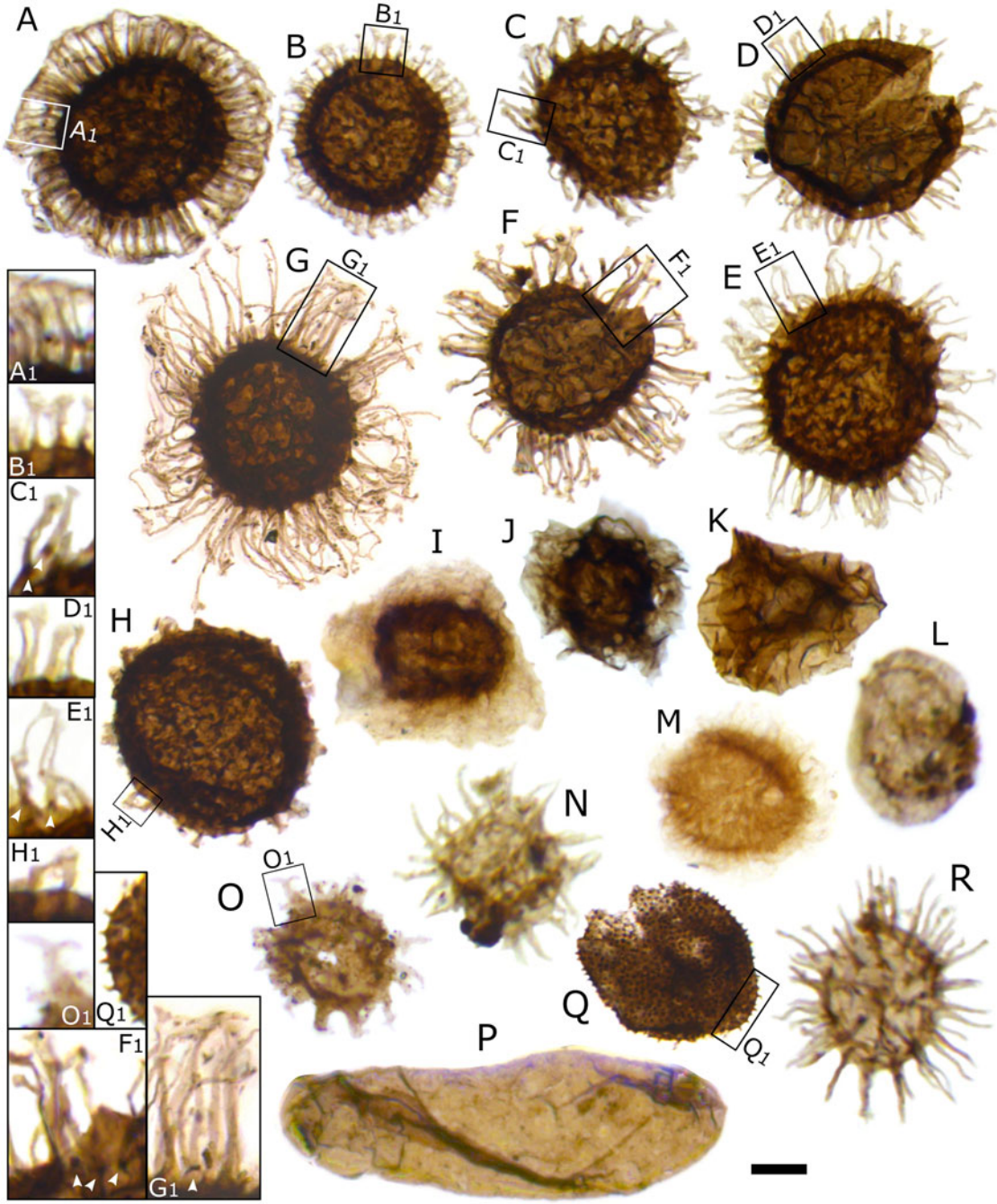

FIGURE 2. Acritarch assemblage from the Buen Formation, Brillesø. A–H, Acritarchs from the *Skiagia*-plexus. Magnified areas show detail of process morphology, with plug-like structures indicated by white arrowheads. A, *Skiagia scottica* Downie, 1982. B, *Skiagia ciliosa* (Volkova, 1969) Downie, 1982 (morphotype A). C, *Skiagia ciliosa* (Volkova, 1969) Downie, 1982 (morphotype B). D, *Skiagia orbiculare* (Volkova, 1968) Downie, 1982. E, *Skiagia compressa* (Volkova, 1968) Downie, 1982. F, *Skiagia ornata* (Volkova, 1968) Downie, 1982. G, *Skiagia* cf. *compressa*. H, *Skiagia* cf. *pura*. I, *Pterospermella velata* Moczydłowska, 1988. J, *Pterospermella solida* (Volkova, 1969) Volkova, 1979 (in Volkova et al. 1979). K, *Cymatiosphaera* cf. *postii*. L, *Granomarginata prima* Naumova, 1960. M, *Comasphaeridium molliculum* Moczydłowska and Vidal, 1988. N, *Goniosphaeridium* cf. *volkovae* Hagenfeldt, 1989. O, *Multiplicisphaeridium dendroideum* (Jankauskas, 1976) Jankauskas and Kirjanov, 1979 (in Volkova et al. 1979), magnified area shows divided process termination. P, *Leiovalia tenera* Kirjanov, 1974. Q, *Lophosphaeridium dubium* (Volkova, 1968) Moczydłowska, 1991, magnified area shows detail of spinose surface sculpture. R, *Heliosphaeridium dissimilare* (Volkova, 1969) Moczydłowska, 1991. Specimens A–N, Q–R are deposited in the Natural History Museum of Denmark, Copenhagen; Specimen O is deposited at the Museum of Evolution, Uppsala, Sweden. Specimens have the following numbers: A, MGUH 33960; B, MGUH 33961; C, MGUH 33962; D, MGUH 33963; E, MGUH 33964; F, MGUH 33965; G, MGUH 33966, H, MGUH 33967; I, MGUH 33968; J, MGUH 33969; K, MGUH 33970; L, MGUH 33971; M, MGUH 33972; N, MGUH 21534; O, PMU 36118-2; P, MGUH 33973; Q, MGUH 33974; R, MGUH 33975. Scale bars, 10 μm; in L, N, R, and magnified areas, 5 μm.

Granomarginata prima (Fig. 2L), which are known from the underlying *Asteridium–Comasphaeridium* and *Skiagia ornata–Fimbriaglomerella membranacea* Zones of Terreneuvian–Cambrian Stage 3 age (Moczydłowska 1991). However, the poorly constrained biostratigraphic and paleogeographic range of these species is being continuously expanded (Landing et al. 2013; Palacios et al. 2018; Slater and Willman 2019; Zheng et al. 2020). The trilobite record at Brillesø includes *Mesolenellus hyperboreus* from the *Olenellus* Zone (Cambrian Stages 3–4), but the lower part of the upper member (locality B1; Fig. 1C) also yielded the nevadiid *Limniphacos perspicullum*. These levels were tentatively correlated with the *Nevadia addyensis* Zone of the Montezuman Stage (Cambrian Stage 3; Hollingsworth 2011; Peel and Willman 2018). The consistent records of acritarchs and trilobites at Brillesø therefore strengthen support for the Cambrian Stages 3–4 age of the oldest pterobranch (Slater et al. 2018) and crustacean (Wallet et al. 2021) fragments that have been recovered as small carbonaceous fossils from the same locality.

Sampled Horizons and Palynological Material

Sampling data are given by Vidal and Peel (1993), Peel and Willman (2018), and Wallet et al. (2021) and are summarized here. Nine palynological preparations corresponding to three samples collected by Grønlands Geologiske Undersøgelse (Geological Survey of Greenland, GGU prefix) from the Brillesø site were processed by Vidal and Peel (1993) using a standard acid maceration procedure (Vidal 1988). GGU sample 184002 was recovered from a 60-cm-thick horizon of iron-stained dark-gray mudstones ("Brillesø locality 1," B1; Fig. 1C) corresponding to the lowermost part of the upper member of the Buen Formation. GGU samples 184003 and 184004 were retrieved from a nearby outcrop of dark-gray mudstones ("Brillesø locality 2," B2; Fig. 1C) stratigraphically 9 m above Brillesø locality 1 and span a bed thickness of 2.1 m and 1 m, respectively. All specimens are deposited in the Natural History Museum of Denmark, Copenhagen; except specimen PMU 36118-2 (Fig. 2O), hosted at the Museum of Evolution, Uppsala, Sweden.

Our palynological analysis revealed a total of six *Skiagia* species (all three samples combined); namely *Skiagia scottica* Downie, 1982, *S. ciliosa* (Volkova, 1969) Downie, 1982, *Skiagia orbiculare* (Volkova, 1968) Downie, 1982, *S. ornata* (Volkova, 1968) Downie, 1982, *Skiagia compressa* (Volkova, 1968) Downie, 1982, and *S.* cf. *pura* Moczydłowska, 1988. Identification was based on original diagnoses (Volkova 1968, 1969; Downie 1982; Moczydłowska 1988) and subsequent taxonomic descriptions (e.g., Knoll and Swett 1987; Hagenfeldt 1989; Vidal and Peel 1993; Moczydłowska 1991, 2011; Vanguestaine et al. 2002; Palacios et al. 2011, 2020). Specimens having long (> ~30% of the vesicle diameter), tubular, and typically numerous (>50) processes were attributed to *S. ornata* (Figs. 2F, 3), while similar vesicles with shorter (~20%–30% of the vesicle diameter) and generally fewer processes were attributed to *S. orbiculare* (Figs. 2D, 3). *Skiagia ciliosa* specimens are represented by two morphotypes in the studied assemblage (Moczydłowska 1991; Vidal and

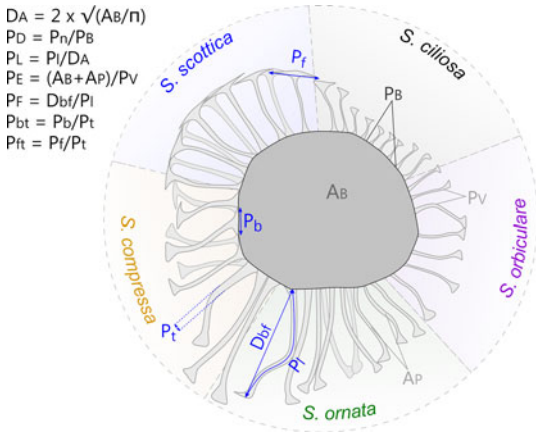

FIGURE 3. Measured parameters and their variations across the five *Skiagia* morphotypes selected for multivariate analyses. D_A: vesicle diameter, calculated from the area of the central body (A_B; i.e., vesicle lacking processes) assuming the circularity of its outline; P_D: process density, calculated as the ratio between process number (P_n) and the length of the process-bearing surface, considered as the entire perimeter of the central body (P_B) in complete vesicles; P_L: size-independent estimator of process length (P_l) measured on the longest, complete process; P_E: process evenness, calculated as the total vesicle area (i.e., sum of the central body area [A_B] and the process area [A_P]) divided by its perimeter (P_V); P_F: process flexibility, calculated as the ratio between the shortest distance from process base to process tip (D_{bf}) and process length (P_l), measured on the most sinuous process; P_{bt}: basal expansion rate, calculated as the ratio between basal process width (P_b) and tubular process width (P_t); P_{ft}: apical expansion rate, calculated as the ratio between the width of the process tip (P_f) and tubular process width (P_t). T_V and P_S were not illustrated here (see main text for detailed explanations).

Peel 1993); specimens from morphotype A have short (< ~20% of the vesicle diameter) and slender processes (Fig. 2B); while specimens from morphotype B exhibit longer (20–30% of the vesicle diameter), more robust processes (Fig. 2C) with distinctively widened bases. Specimens having long (> ~30% of the vesicle diameter) processes with a widened base, imparting an irregular outline to the vesicle, were identified as *S. compressa* (Figs. 2E,G, and 3). Specimens referred to as *S.* cf. *pura* differ from *S. pura* Moczydłowska, 1988 in having shorter and less numerous processes, but share their broad funnel-shaped morphology (Fig. 2H).

Specimens were photographed under light microscopy at a range of focal depths and measured from stacked images using the software ImageJ. Measurements were obtained from a total of 191 specimens, including 82 specimens of *S. scottica*, 42 specimens of *S. ciliosa*, 25 specimens of *S. orbiculare*, 24 specimens of *S. ornata*, and 18 specimens of *S. compressa*. *Skiagia ciliosa* morphotypes A and B were not distinguished in this study owing to the known overlap in their disparity (Moczydłowska 1991). *Skiagia pura* specimens were too rare to be usefully included in the analysis.

Methods

A total of 10 parameters were measured in *Skiagia* specimens from all three samples, forming the basis of our multivariate analyses. Independent counts of life cycle structures in all five *Skiagia* species were performed on a separate collection of specimens from the same palynological preparations as those used for the main morphometric study. A detailed description of measured parameters, ordination techniques, and life cycle analysis is given below.

Measured Parameters.—Among the selection of 10 parameters used in this morphometric study, 7 were chosen to reflect the original diagnoses of *Skiagia* species (Volkova 1968, 1969; Downie 1982; Moczydłowska 1991; Fig. 3): process density (P_D), process length (P_L), process evenness (P_E), width of the tubular process (P_t), basal expansion rate (P_{bt}), apical expansion rate (P_{ft}), and process solidity (P_s). Process density is the ratio between the number of processes protruding from the central body (P_n) and the length of the process-bearing surface (equivalent to the perimeter of the central body P_B if the entire vesicle is preserved). The length of processes (P_L) was measured on the longest fully observable process, from base to tip, and divided by the vesicle diameter (D_A, see below) to remove overall size dependence. Process evenness (P_E) was calculated as the area/perimeter ratio of entire specimens and measures the degree of indentation of their outline. This parameter captures the propensity of processes to join each other at the tip, a typical feature of *Skiagia scottica* (Downie 1982; Moczydłowska 1991). However, when processes are loose, P_E is expected to be dependent on other features such as process density, flexibility, and length. Area ($A_B + A_P$) and perimeter values (P_V) were automatically calculated from binary images following consistent thresholding of all photographs ($T = 238$),

hence P_E may also partly depend on the thickness of the wall, as the lightest portions of vesicle fall beyond the threshold value. The width of the tubular process (P_t) was measured from the tubular portion of the processes, between the conical base and funnel-shaped tip. The basal expansion rate (P_{bt}) is defined here as the ratio between the width of the conical base (P_b) and the width of the tubular process (P_t), while the apical expansion rate (P_{ft}) is the ratio between the width of the funnel-shaped process termination (P_f) and the width of the tubular process (P_t). Both P_b and P_f were measured on the widest bases and funnels, respectively. Process solidity (P_s) is the ratio between the pixel intensity value of the central body wall (T_V, see below) and the pixel intensity value of the process wall. This parameter captures the color difference between the central body and processes, which features in original descriptions of *S. ciliosa* (Volkova 1969).

The remaining three parameters retained for quantitative study represent auxiliary features of unknown (or unrecognized) taxonomic potential (Fig. 3); namely, vesicle size (D_A), process flexibility (P_F) and the thickness of the vesicle wall (T_V). These parameters are used to explore the full disparity of *Skiagia* and prospect for additional descriptors of between-species variation. The vesicle size was calculated as the diameter of a circle of the same area as the central body (A_B). Process flexibility (P_F) was measured on the most sinuous process and calculated as the distance from process base to process tip (D_{bf}) divided by process length (P_L). The thickness of the vesicle wall (T_V) was estimated from the pixel intensity value measured in the lightest area of the central body, devoid of fractures or inner body, and was divided by the intensity value of a white pixel (255).

A few other characters featuring in previous descriptions of *Skiagia* species are not represented in the set of 10 parameters considered in this study, either because of their questionable systematic value and/or a lack of suitable measurement protocols. These include the basal plug of *S. ciliosa*, which is commonly recognized as a key diagnostic feature of the taxon (Moczydłowska 1991; Palacios et al. 2020) but has not been formally described in its original diagnosis (Volkova 1969). Repeated observations of plug-like structures in other *Skiagia* species (Downie 1982; Hagenfeldt 1989; Zang 2001; Moczydłowska 2011; Fig. 2E–G) cast doubt on the taxonomic reliability of this character, while its recognition beyond the thick-walled central body and/or within narrow processes is partly subjective. Similarly, the presence or absence of walls between processes and the central body cavity (Moczydłowska 2011) was not considered in this analysis owing to the scarcity of observable data (and the impracticality of obtaining such data in most palynological studies). The morphology of process tips and bases is widely used to distinguish species of the genus *Skiagia*. In particular, processes in *S. scottica* have been described as being cylindrical and particularly flat at the tip (Moczydłowska 1991, 2010), while *S. compressa* has conical process bases imparting a wavy outline to the central body (Moczydłowska 1991; Palacios and Moczydłowska 1998). Considering the large intraspecific disparity of both process tips (Downie 1982; Vanguestaine et al. 2002) and bases (Knoll and Swett 1987; Vidal and Moczydłowska 1996; Moczydłowska 2011), together with their high susceptibility to taphonomic alteration and specimen orientations, these parameters and their variation seem to be best captured by simple, standardized measurements of width (P_{bt} and P_{ft}; Fig. 3) rather than categorical variables or more advanced semilandmark- and landmark-based analyses (e.g., Lohmann 1983; Sheets et al. 2004). The outline of the central body is often described as being circular or oval (e.g., Volkova 1968, 1969; Moczydłowska 1991; Zang 2001), which can be quantified by a measure of eccentricity. However, this parameter was found to contribute very little to variation along the first three principal components (loadings < 0.15) and was therefore discarded from the analysis.

All measurements (P_D, P_L, P_E, P_t, P_{bt}, P_{ft}, P_s, D_A, P_F, T_V; Fig. 3) were performed using the free software ImageJ (Schneider et al. 2012; Rueden et al. 2017) and its Shape Smoothing plug-in (used to remove noise after thresholding). Incomplete or opened vesicles were analyzed on a single portion, which was pasted over missing parts. All values were

standardized by subtracting the mean and dividing by the standard deviation to account for scale differences between parameters.

Multivariate Analyses of Morphological Parameters.—Principal component analysis (PCA) was used to explore the overall disparity of the studied assemblage and determine whether consistent groupings can be recognized beyond any sources of intraspecific variation. The taxonomic subdivision of the genus *Skiagia* was then assessed using linear discriminant analysis (LDA), which maximizes between-group variance (e.g., Albrecht 1980; Campbell and Atchley 1981; Strauss 2010; Huntley 2011). This ordination technique has been widely used in paleontology to help discriminate species based on morphological criteria in groups as varied as sharks (Marramà and Kriwet 2017), killifish (Reichenbacher et al. 2007), plants (Álvarez et al. 2009), bees (De Meulemeester et al. 2012), bryozoans (Cheetham 1986), mollusks (Geary 1992; Marko and Jackson 2001; Reyment 2003), trilobites (Labandeira and Hughes 1994), and brachiopods (Kowalewski et al. 1997; Carranza and Carlson 2021). LDA has also been used as a quantitative tool for taxonomic revision of various upper Cambrian and Ordovician acritarch taxa (Wang et al. 2017; Yan et al. 2017; Kroeck et al. 2020).

It is worth noting that an inherent degree of circularity is to be expected when using LDA for taxonomic purposes, as a priori groupings are defined based on criteria that are identical to those used for the calculation of discriminant functions (Huntley 2011). In the case of *Skiagia*, a priori group attribution is inevitably subjective to some degree, because established *Skiagia* species were not originally defined on quantitative grounds and transitional forms are evident in their populations. For these reasons, LDA was performed on a reduced dataset of 83 "unambiguous" specimens that could be assigned to a given species using the currently defined criteria with a reasonable degree of confidence. The remaining 108 specimens (categorized as "ambiguous"), which did not obviously fall into one or another of the established *Skiagia* species, were classified a posteriori using the discriminant functions regardless of their tentative species attribution. The boundary between unambiguous and ambiguous specimens was defined arbitrarily in order to achieve a reasonable trade-off between dataset quality and size. This approach was intended to calibrate the ordination plot with systematically defined characters, reducing any background noise created by poorly preserved and/or transitional forms.

LDA of the entire dataset ($N = 191$; "ambiguous" specimens being tentatively attributed to one species) was also performed to estimate the proportion of correct classifications in a more realistic situation in which ambiguous and/or transitional morphologies form a substantial portion of the microfossil assemblage. The statistical significance of observed between-species variations was tested using permutational multivariate analysis of variance, a nonparametric alternative to multivariate analysis of variance testing the difference between multivariate means (Anderson 2017). Significance calculations were based on the Mahalanobis distance between species, which accounts for correlations between variables (Campbell and Atchley 1981; McLachlan 1999).

All multivariate analyses were performed using the software package PAST (Hammer et al. 2001; Hammer and Harper 2006). Separate LDAs and PCAs were run for each of the three studied samples to test for any potential paleoenvironmental and/or small-scale temporal effects on observed patterns. All PCAs were conducted on variance–covariance matrices.

Quantitative Analysis of Life Cycle Structures.—Two hundred fifty well-preserved and identifiable *Skiagia* specimens were randomly selected in each of the three samples to investigate the distribution of life cycle stages among *Skiagia* species. Discrete features related to encystment (i.e., internal bodies; Moczydłowska 2010, 2016) and excystment (i.e., opened vesicles) were counted, and their relative frequency was calculated for each *Skiagia* species. The distribution of those features among distinct samples was also analyzed.

Results

Principal Component Analysis

PCA of the entire dataset exhibits a remarkable spread over the first four components

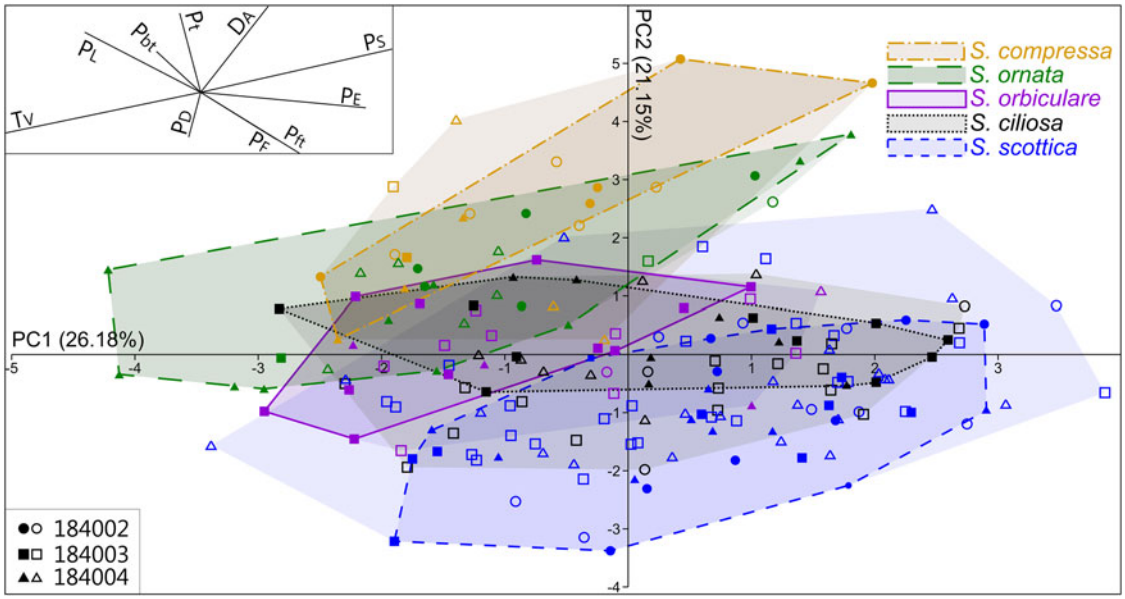

FIGURE 4. Results of the principal component analysis (PCA) showing variation across the first two PCs. The entire *Skiagia* dataset has been included ($N = 191$). The proportion of variation explained by each PC is shown along its respective axis. Filled and empty symbols represent unambiguous and ambiguous specimens, respectively, and are color coded according to their (tentative) species attribution. Inset on the upper left corner shows the PC 1–PC 2 biplot. Abbreviations for parameters are provided in the caption for Fig. 3.

(Figs. 4, 5). PC 1 accounts for just 26.2% of overall variation and is chiefly driven by T_V, P_S, and P_E (Fig. 5B). The contribution of PC 2 to total variation is slightly lower (21.1%) and driven by a complex combination of parameters, including D_A, P_t, P_L, and P_{ft} (Fig. 5C). PC 3 and PC 4 explain 13.1% and 10.4% of overall variance, respectively, chiefly reflecting the contribution of P_D and P_t (Fig. 5D,E). The PC 3–PC 4 ordination plot is devoid of any obvious pattern (Supplementary Fig. 1) and does not warrant further analysis. Significant correlations were found between parameters (Supplementary Table 1), most notably P_S, which is negatively correlated with T_V (Spearman's rank correlation coefficient $[r_s] = -0.97$; $p < 0.001$). Moderate correlations exist between P_E and other parameters, including P_L ($r_s = -0.41$; $p < 0.001$), P_{ft} ($r_s = 0.45$; $p < 0.001$), and T_V ($r_s = -0.46$; $p < 0.001$); and between D_A and P_D ($r_s = -0.42$; $p < 0.001$).

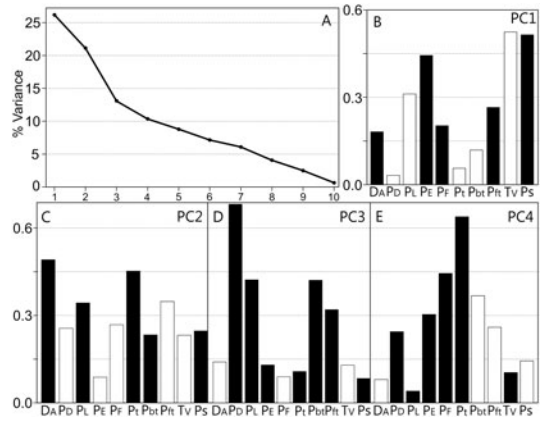

FIGURE 5. Scree plot and loadings of the principal component analysis (PCA) performed on the entire *Skiagia* dataset ($N = 191$). A, Scree plot showing the percentage of variance explained by each PC. B–E, loadings associated with each PC showing positive and negative coefficients as black and white bars, respectively. Abbreviations for parameters are provided in the caption for Fig. 3.

Intraspecific variation is mostly captured by PC 1, which is chiefly driven by two negatively correlated variables, T_V and P_S (Fig. 5B). This echoes the broad and overlapping range of these parameters in all five *Skiagia* species (Fig. 6I,J). Between-species variance seems better expressed by PC 2, although no specific groupings are visible (Fig. 4). Instead, a continuous gradient of forms ranging from *Skiagia scottica* to *Skiagia compressa* is detectable from

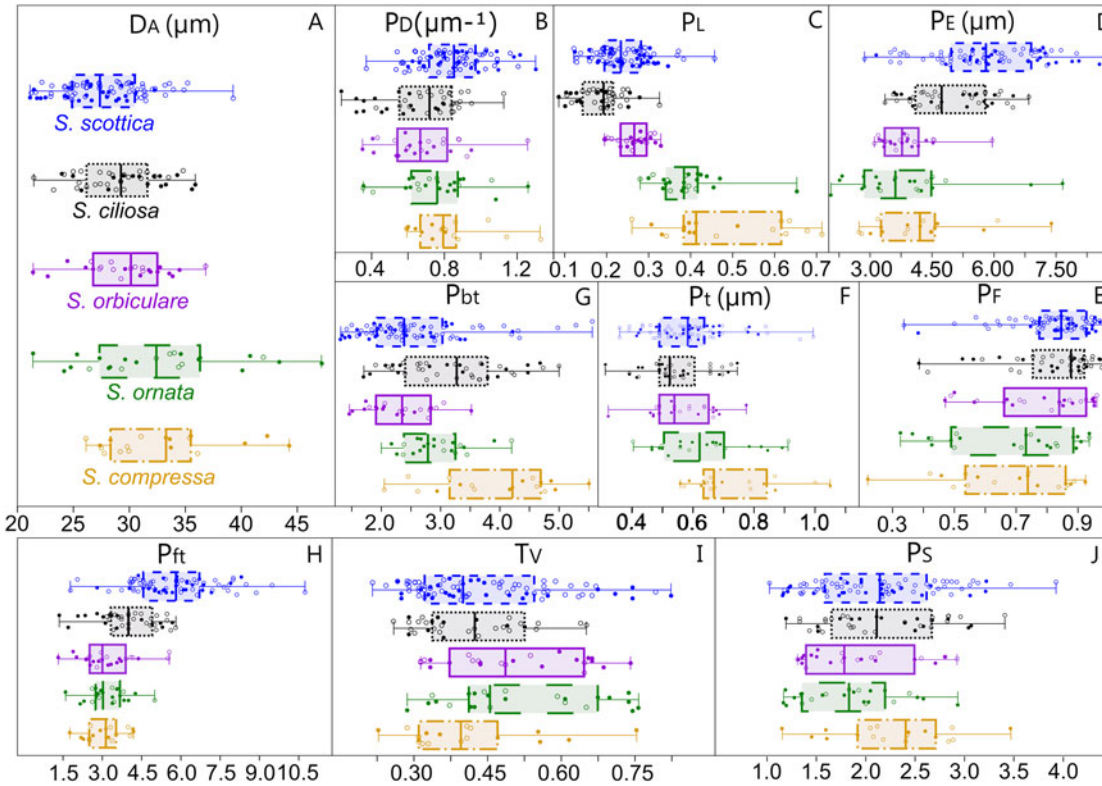

FIGURE 6. Box plots and scatter plots showing the distribution of measured parameters among *Skiagia* species. A, Vesicle diameter (D_A, in μm); B, process density (P_D, in number of processes per μm); C, process length (P_L); D, process evenness (P_E, in μm); E, process flexibility (P_F); F, width of the tubular process (P_t, in μm); G, basal expansion rate (P_{bt}); H, apical expansion rate (P_{ft}); I, vesicle thickness (T_V); J, process solidity (P_S). Filled and empty circles represent unambiguous and ambiguous specimens, respectively.

the lower to the upper part of the ordination plot. The exact morphological relationships between the species of this gradient are obscured by extended areas of overlaps and slight compositional differences between samples (Fig. 7, Supplementary Fig. 2). For instance, a more distinct sequence of clearly separated species is observed along the first component in the lowermost sample (GGU sample 184002; Figs. 1C, 7A), reflecting the contribution of P_L, D_A, P_t, and P_{bt}. The clear separation between groups in GGU sample 184002 is likely an artifact resulting from the scarcity of available measurements for *Skiagia ciliosa* and *Skiagia orbiculare*, which occupy a substantial portion of the morphospace between *S. scottica* and *Skiagia ornata* when all samples are included (Fig. 4). Similarly, the scarcity of measurements for S. *compressa* and *S. ornata* in sample 184003 likely explains their overlapping range with other species. The distribution of samples in the ordination plot shows extended areas of overlap (Supplementary Fig. 2) devoid of obvious pattern, suggesting that all levels capture the same morphological spectrum bounded by *S. scottica* and *S. compressa*.

Linear Discriminant Analysis

LDA of unambiguous specimens ($n = 83$; Fig. 8) clarifies the morphological gradient identified using PCA by inflating between-group variance. The LDA plot of the first two discriminant functions (>95% of total variance between groups) shows a continuous sequence of *Skiagia* species from the left to the right end of the ordination plot; namely *S. scottica*, *S. ciliosa*, *S. orbiculare*, and *S. compressa*/*S. ornata*. The latter two species share most of their total morphological range, but unambiguous specimens show better separation, falling toward the top right

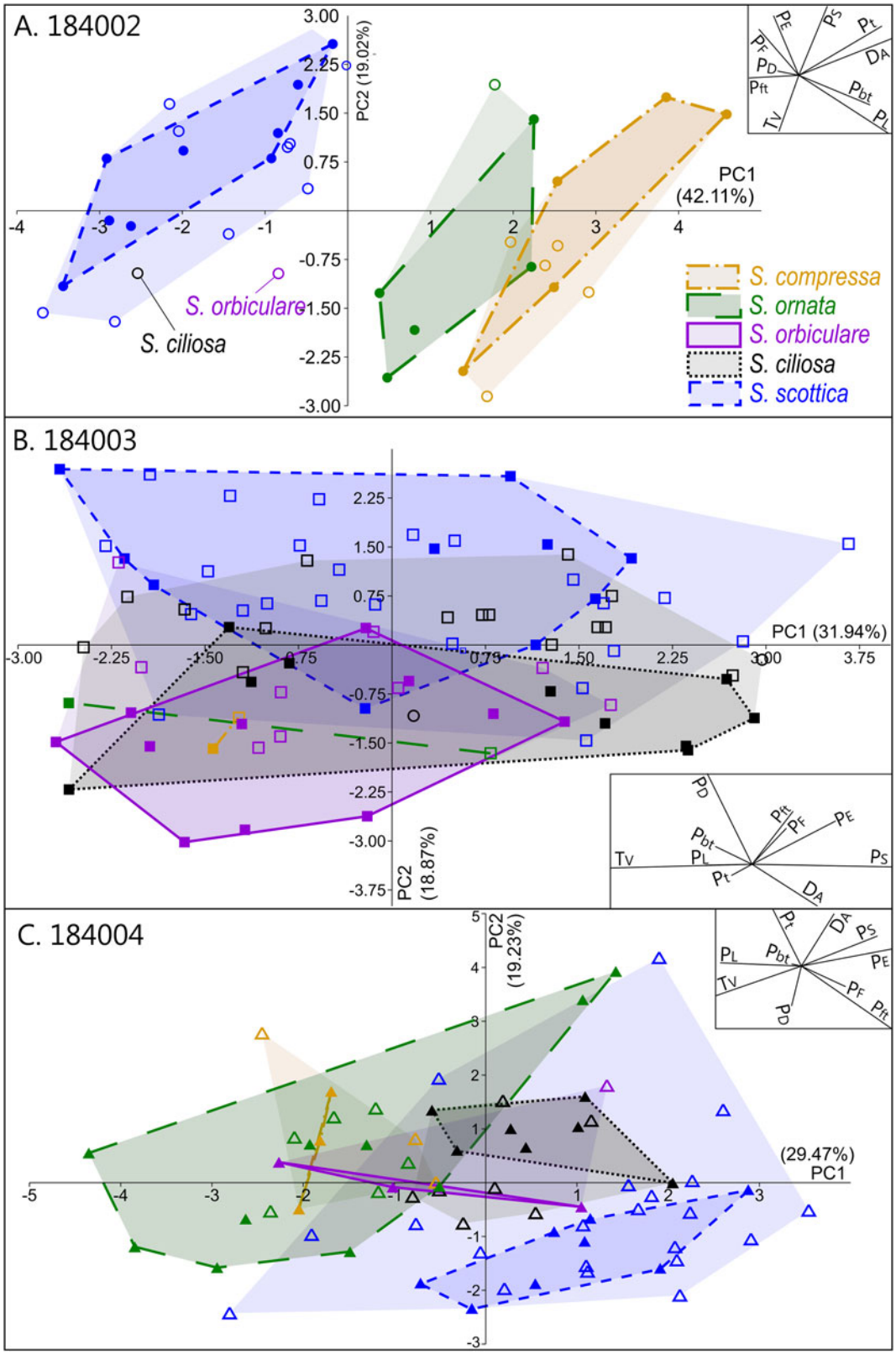

FIGURE 7. Results of the principal component analysis (PCA) in each sample, showing variation across PC 1 and PC 2. A, GGU sample 184002 ($n = 36$); B, GGU sample 184003 ($n = 86$); C, GGU sample 184004 ($n = 69$). The proportion of variation explained by each PC is shown along its respective axis. Filled and empty symbols represent unambiguous and ambiguous specimens, respectively, and are color coded according to their (tentative) species attribution. PC 1–PC 2 biplots are shown as insets on each ordination plot.

region of the morphospace for *S. ornata* and the middle right region for *S. compressa*. Patterns of morphological variation between species are broadly conserved across all three samples (Supplementary Fig. 4), in spite of their slight differences in taxonomic composition (Supplementary Figs. 5, 7).

Although some degree of between-group separation is visible, there exist distinct areas of overlap between all five species. In total, 92.77% of unambiguous specimens were predicted to be assigned correctly to their given groups using jackknife resampling (Lance et al. 2000; Table 1). *Skiagia scottica* was the most robustly classified species (100% correct group attributions), followed by *S. ciliosa* (94.44%), *S. orbiculare* (92.31%), *S. compressa* (87.50%), and *S. ornata* (82.35%). The predicted rate of successful classifications dropped sharply after inclusion of ambiguous forms ($N = 191$), falling below 70% for *S. ciliosa*, *S. ornata*, and *S. orbiculare*. The addition of ambiguous specimens to the ordination plot did not substantially alter patterns of within- and between-group variation, but increased the size of overlapping areas, particularly between *S. ciliosa* and *S. orbiculare* and between *S. ornata* and *S. compressa* (Supplementary Fig. 6). Two regions of the ordination plot are occupied by the range of three different species, namely *S. scottica–S. ciliosa–S. orbiculare* and *S. orbiculare–S. ornata–S. compressa*. In spite of their broad, overlapping morphospace occupation, the multivariate means of each of the five *Skiagia* species were found to be significantly different from one another ($p < 0.01$).

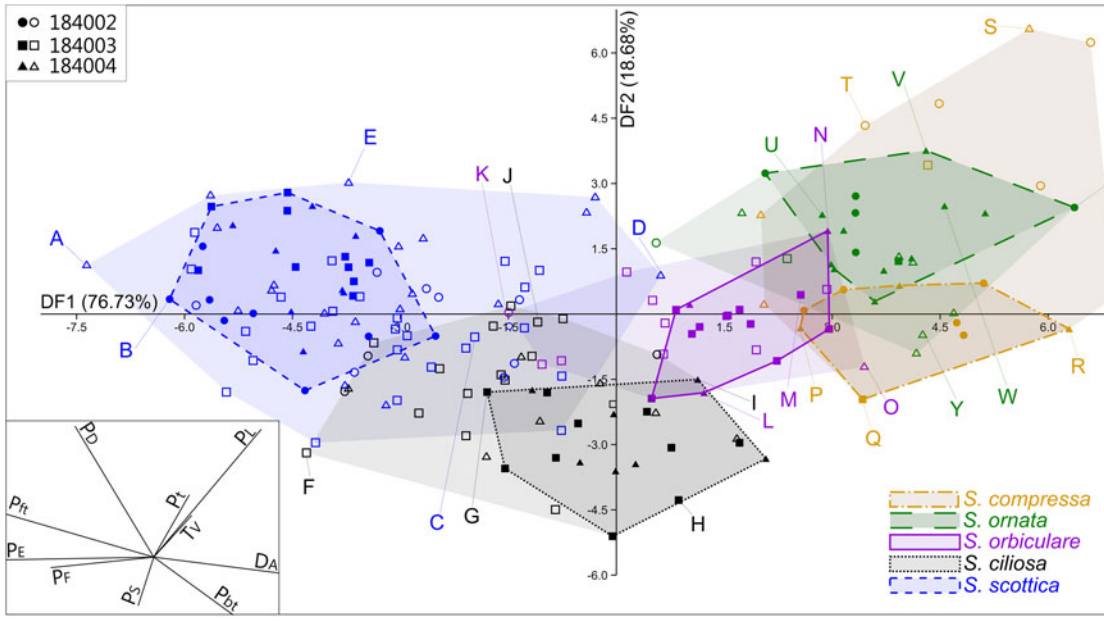

FIGURE 8. Linear discriminant analysis (LDA) of the reduced *Skiagia* dataset, consisting of 83 unambiguous specimens grouped per species. The remaining 108 ambiguous specimens are represented as empty symbols and light-colored convex hulls, color coded according to their tentative species attribution. Ambiguous specimens were plotted a posteriori using discriminant functions calculated from unambiguous specimens. Inset on the bottom left corner shows the DF 1–DF 2 biplot. The proportion of between-group variance explained by each discriminant function (DF) is shown along its respective axis. Specimens in A–Y are illustrated in Fig. 9. Abbreviations for parameters are provided in the caption for Fig. 3.

TABLE 1. Percentage of correct classifications predicted by jackknife resampling, using all specimens ($N = 191$), unambiguous specimens only ($n = 83$), the full set of $g = 5$ species (*Skiagia scottica*, *Skiagia ciliosa*, *Skiagia orbiculare*, *Skiagia ornata*, and *Skiagia compressa*) or $g = 4$ species (*S. scottica*, *S. ciliosa*, *S. orbiculare*, *S. ornata*/*S. compressa*). JCS, jackknife classification success (%).

	JCS ($n = 83$) $g = 5$	JCS ($N = 191$) $g = 5$	JCS ($n = 83$) $g = 4$	JCS ($N = 191$) $g = 4$
S. scottica	100.00	91.67	100.00	91.67
S. ciliosa	94.44	66.00	88.24	67.35
S. orbiculare	92.31	65.38	68.75	65.63
S. ornata	82.35	64.29		
S. compressa	87.50	73.33		
S. ornata/S. compressa			95.65	97.37
Total	92.77	75.92	90.36	82.20

The distribution of *Skiagia* species in the ordination plot is chiefly governed by a complex combination of characters including P_E, P_{ft}, P_L, P_D, D_A, and P_F (Supplementary Fig. 3). *Skiagia scottica* is defined by its high P_{ft}, P_D, and P_E values (Fig. 6B,D,H), as is expected from its numerous processes connected to each other by their wide, funnel-shaped termination (Fig. 3). The large number and apical morphology of processes in *S. scottica* may also explain its relatively high P_F values (Figs. 6E, 8), as process attachment may have contributed to maintaining an evenly spread network of straight processes resistant to bending and deformation. *Skiagia ciliosa* partly diverges from this group, with morphotype A specimens having fewer and shorter processes gathering toward the left and lower portions of the ordination plot (Figs. 8, 9F–H). Morphotype B specimens fall closer to the morphological range of *S. orbiculare* (Fig. 8), which reflects their comparable process lengths but distinct process morphologies at the base (Figs. 6C,G, and 9I). Specimens attributed to *S. orbiculare* share numerous features with both *S. scottica* and *S. ciliosa* (Figs. 6, 8), but have lower P_E values on average (Fig. 6D), and slightly longer processes with narrower tips (Figs. 6C,H, and 9M–O). *Skiagia ornata* and *S. compressa* are better distinguished from other *Skiagia* species, being characterized by longer processes (Figs. 6C, 9Q–Y) and generally larger vesicle size (Fig. 6A). *Skiagia compressa* differs from *S. ornata* only by having larger P_t (Fig. 6F) and P_{bt} values (Figs. 6G, 9P–T). Moreover, a few *S. compressa* specimens form distinct outliers gathering toward the upper right-hand portion of the ordination plot (Fig. 8), resulting in substantial overlaps with the *S. ornata* population. These specimens have unusually long processes (>50% of the vesicle diameter) with moderately expanded bases (Figs. 2G, 9S), which may conform to the diagnosis of either *S. ornata* or *S. compressa*. Considering these two species as synonymous in the present setting, 97.37% of specimens assigned to this group (both ambiguous and unambiguous) were predicted to be classified correctly after jackknife resampling.

Overall, the morphological range of *S. scottica* is best defined by P_{ft} and P_E, while P_L chiefly governs the trend from *S. ciliosa* to *S. ornata*/*S. compressa*. While a number of other parameters appear to be useful descriptors of between-species variation (e.g., D_A, P_F, P_{bt}), the ability of T_V and P_S to capture differences between *Skiagia* species seems to be limited in the current setting (Figs. 4, 6, Supplementary Fig. 3).

Quantitative Analysis of Life Cycle Structures

Various developmental stages have been identified in the studied *Skiagia* population, being chiefly evidenced by the presence of excystment (opened vesicles) and encystment structures (vesicles enclosing an internal body; Moczydłowska 2010, 2016; Fig. 10). Potential outer membranes have been recognized as optically faint, light-colored, but clearly delineated agglomerations of structureless organic matter between the processes of a few *S. scottica* specimens (Fig. 10A) and transitional forms between *S. scottica* and *S. ciliosa* (Fig. 10B,C). These structures have not been retained for quantitative study owing to their scarcity and the likelihood of confusion between the widely flaring tips of *S. scottica* and any potential overlying, thin-walled membrane.

Internal bodies can be divided into two groups: dark to opaque, clearly defined subrounded structures (Fig. 10K,L) similar to previously described endocysts (e.g., Zang et al. 2007: figs. 12A,D, and 14A,B,D; Moczydłowska 2010); and more translucent, lighter-colored subspherical bodies (Fig. 10M,N). Translucent endocysts in *Skiagia* have previously been

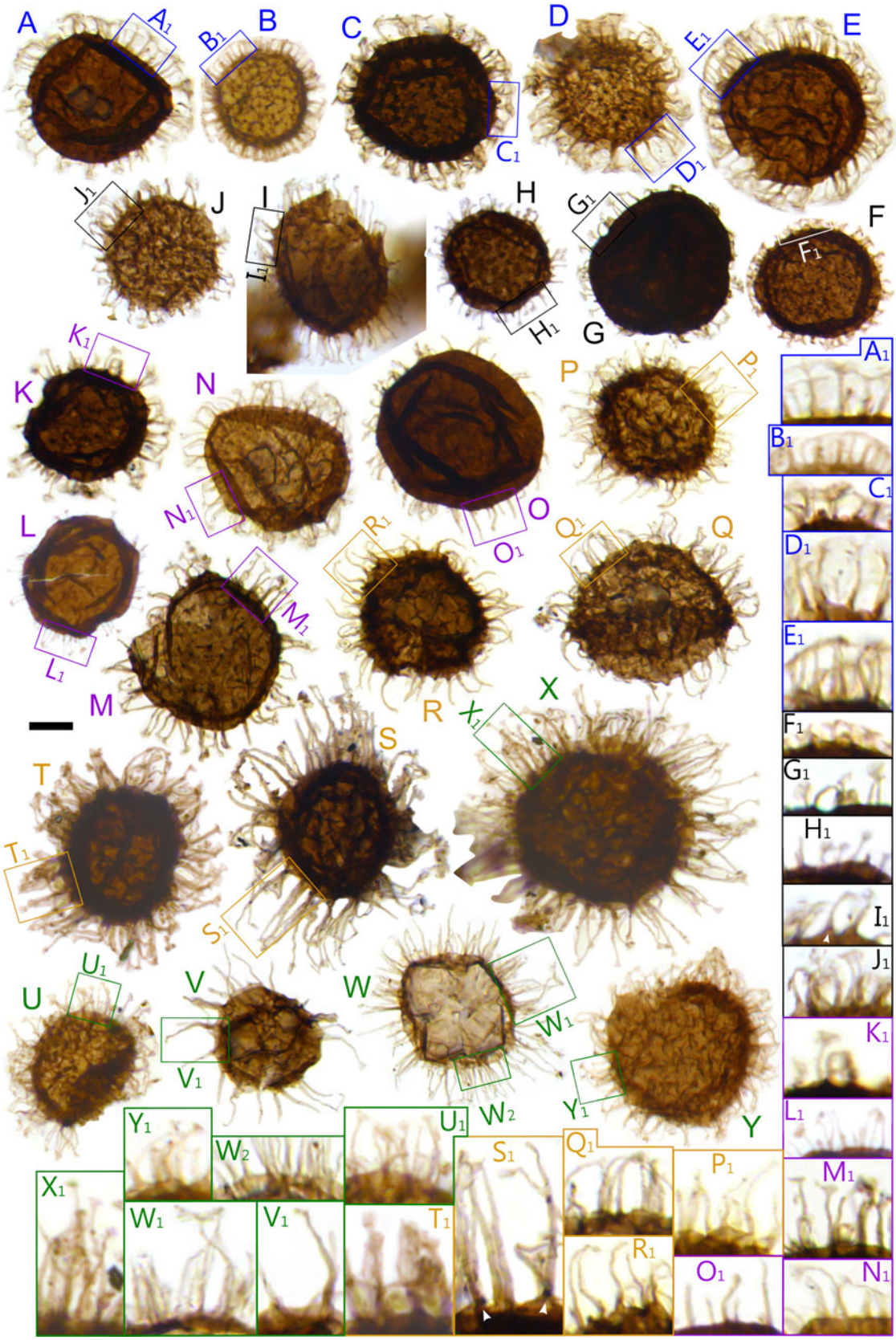

FIGURE 9. Selection of *Skiagia* specimens from the LDA plot (Fig. 8). Magnified areas show detail of process morphologies. A–E, *Skiagia scottica*; F–J, *Skiagia ciliosa*; K–O, *Skiagia orbiculare*; P–T, *Skiagia compressa*; U–Y, *Skiagia ornata*. All specimens are deposited in the Natural History Museum of Denmark, Copenhagen, and have the following numbers: A, MGUH 33976; B, MGUH 33977; C, MGUH 33978; D, MGUH 33979; E, MGUH 33980; F, MGUH 33981; G, MGUH 33982; H, MGUH 33983; I, MGUH 33984; J, MGUH 33985; K, MGUH 33986; L, MGUH 33987; M, MGUH 33988; N, MGUH 33989; O, MGUH 33990; P, MGUH 33991; Q, MGUH 33992; R, MGUH 33993; S, MGUH 33994; T, MGUH 33995; U, MGUH 33996; V, MGUH 33997; W, MGUH 33998; X, MGUH 33999; Y, MGUH 34000. Scale bars, 10 μm; in magnified areas, 5 μm.

reported from the thermally unaltered Lükati Formation (Estonia; Moczydłowska 2010), but are easily confused with circular series of compression folds or shriveled cytoplasm. The translucent endocysts included in this analysis differ from compression folds in showing higher optical density than the surrounding vesicle at any point within the outline of the inner body (Fig. 10M,N).

Dark to opaque endocysts were largely restricted to the *S. compressa* population (Fig. 11, Supplementary Table 2) and completely absent in vesicles attributed to *S. scottica* and *S. orbiculare*. Overall encystment rate (proportion of internal bodies, either dark or translucent) was found to be increasing throughout the *S. scottica–S. ornata/S. compressa* morphological gradient (Fig. 11A), being null in *S. scottica*, extremely low in *S. ciliosa* and *S. orbiculare* (1.29% and 1.25%, respectively), intermediate in *S. ornata* (3.21%), and highest in *S. compressa* (9.4%; Supplementary Table 2). The scarcity of inner bodies inevitably leads to differences in counts between individual samples (Fig. 11B); however, the encystment rate was found to be invariably highest in *S. compressa*.

Excystment structures have been observed in all five *Skiagia* species but were found to be invariably rarest in the *S. ornata* population (Fig. 11), occurring in just 15.38% of vesicles. Opened vesicles were also relatively rare in the studied *S. compressa* population (17.67% on average). The excystment rate was found to increase from *S. scottica* to *S. orbiculare* (Fig. 11A), thereby replicating observed patterns of between-species variation (Fig. 8, Supplementary Fig. 6). GGU sample 184002 exhibits a slightly different excystment pattern (Fig. 11B), with *S. ciliosa* showing the highest proportion of opened vesicles.

Despite slight differences in taxonomic composition between sampled levels (Fig. 1C; Supplementary Fig. 7), total encystment and excystment rates were found to be similar in all three samples, ranging from 3.2% to 5.6% for the former and 20.8% to 25.2% for the latter (Supplementary Table 2).

Discussion

Multivariate morphometric analysis of *Skiagia*-plexus acritarchs from North Greenland revealed an uninterrupted spectrum of forms between five morphospecies: *Skiagia scottica*, *Skiagia ciliosa*, *Skiagia orbiculare*, *Skiagia compressa*, and *Skiagia ornata*. Importantly, the main aspects of this pattern are captured by all studied samples using LDA, PCA, and an independent analysis of encystment and excystment structures, demonstrating its robustness to the uncertainties of group attribution and any potential small-scale paleoenvironmental and/or stratigraphic variations. The absence of obvious morphological clustering across the studied sequence of *Skiagia* species suggests that (1) the species-level subdivision of the genus *Skiagia* is arbitrary and questions its use in biostratigraphy; (2) a mixture of ontogenetic, taphonomic, paleoenvironmental, and paleoecological factors likely control the morphospace occupation of *Skiagia* acritarchs; and (3) *Skiagia* species counts do not offer an impartial measure of morphological or taxonomic diversity.

A Morphometric Approach to Clarifying *Skiagia* Form Taxonomy and Its Biostratigraphic Applications

Our analysis has revealed extended areas of overlap between *Skiagia* species, accounting for as much as ca. 35% misclassifications in *S. ornata* and *S. orbiculare* (Table 1). Intermediate morphotypes have been recognized previously within the genus *Skiagia*, including between *S. ornata* and *S. orbiculare*, *S. ciliosa* and *S. compressa*, and across the *S. scottica–S.*

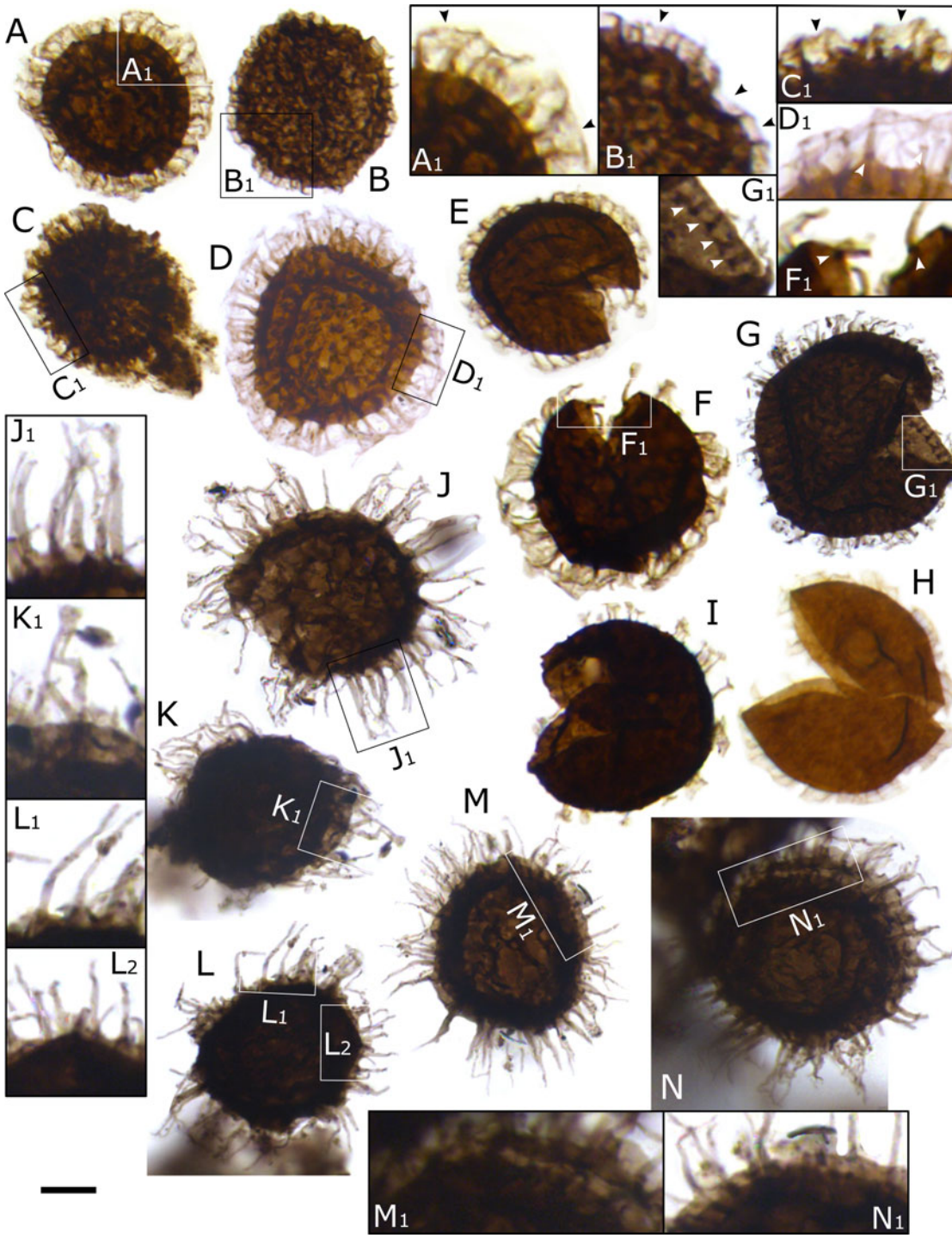

FIGURE 10. Life cycle structures among *Skiagia* species. A–C, possible outer membranes (black arrowheads) in *Skiagia scottica* (A) and transitional forms between *S. scottica* and *Skiagia ciliosa* (B, C). D, Closed *S. scottica* vesicle. E–J, Opened vesicles attributed to *S. scottica* (E, F), transitional forms between *S. scottica* and *S. ciliosa* (G, H), *S. ciliosa* (I), and *Skiagia compressa* (J). K, L, Dark to opaque inner bodies in vesicles attributed to *Skiagia ornata* (K) and *S. compressa* (L). M, N, Translucent inner bodies in transitional forms between *S. compressa* and *S. ornata*. White arrowheads point to plug-like structures. All specimens are deposited in the Natural History Museum of Denmark, Copenhagen, and have the following numbers: A, MGUH 34001; B, MGUH 34002; C, MGUH 34003; D, MGUH 34004; E, MGUH 34005; F, MGUH 34006; G, MGUH 34007; H, MGUH 34008; I, MGUH 34009; J, MGUH 34010; K, MGUH 34011; L, MGUH 34012; M, MGUH 34013; N, MGUH 34014. Scale bars, 10 μm; in magnified areas, 5 μm.

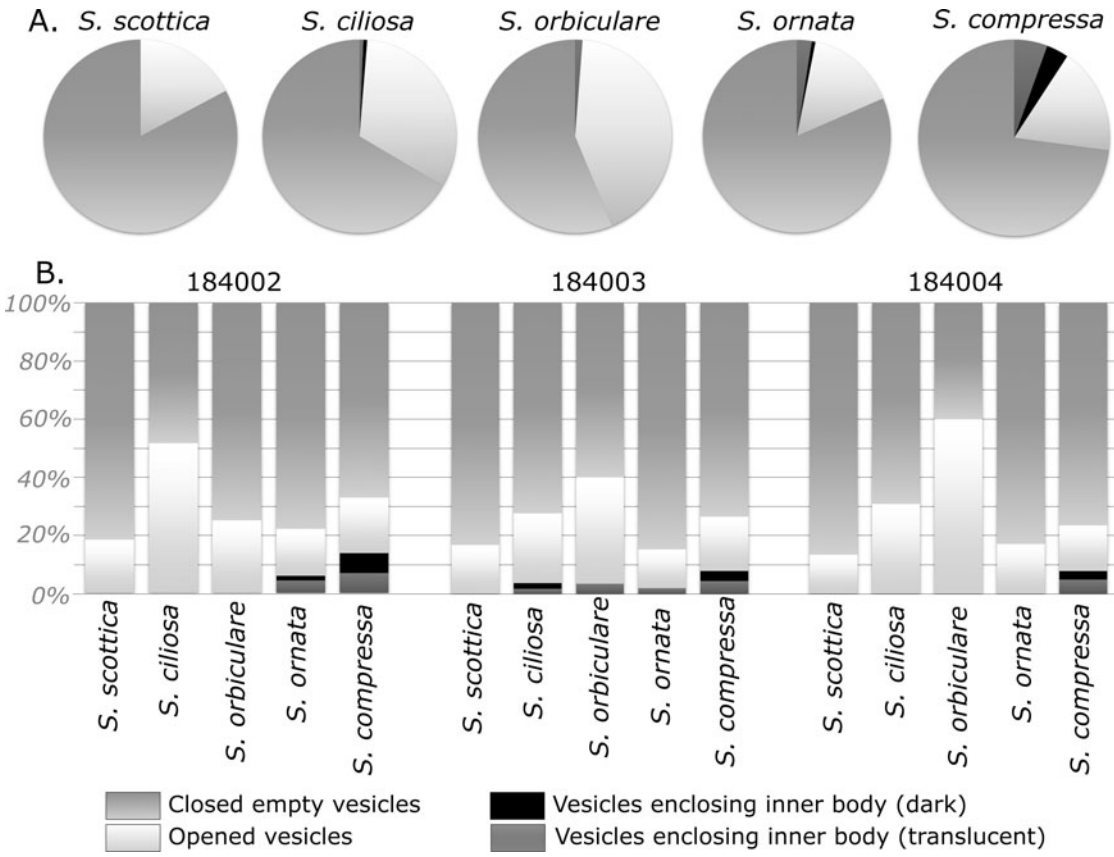

FIGURE 11. Distribution of life cycle structures among *Skiagia* species. A, Pie charts of life cycle structures in *Skiagia scottica* ($n = 93$), *Skiagia ciliosa* ($n = 155$), *Skiagia orbiculare* ($n = 80$), *Skiagia compressa* ($n = 266$), and *Skiagia ornata* ($n = 156$); all samples combined ($N = 750$). B, Stacked charts of life cycle structures among species in GGU samples 184002, 184003, and 184004; 250 specimens were counted in each sample. Raw data are available in Supplementary Table 2.

ornata–S. compressa plexus (Moczydłowska 1991; Moczydłowska and Willman 2009). This study builds upon these observations, shedding light on the extent and origins of within-species and between-species variance. The clear difference between LDA and PCA ordination patterns implies that form species have not been defined based on directions of maximum variance, which appears to be largely driven by parameters susceptible to thermal alteration (T_V, P_S; Figs. 4, 5). Instead, the species-level subdivision of *Skiagia* discretizes a continuous morphological sequence driven by a subtle combination of parameters more or less susceptible to fragmentation and deformation (Figs. 6, 8). Among those, widely used diagnostic features such as P_L, P_{ft}, or P_{bt} were shown to be important descriptors of variation between individual species in the current setting, but are also usefully complemented by subordinate characters that do not feature prominently in *Skiagia* diagnoses; namely, D_A, P_D, P_E, P_F, and P_t. Regardless of the exact origins of observed intra- and interspecific disparity, the absence of clear groupings within the morphological range of *Skiagia* points to the arbitrariness of species-level taxonomic boundaries, which have yet to be defined on a morphometric basis.

Although care has been taken to select the best-preserved specimens, the effect of taphonomy on these patterns is likely to be important, not least given the susceptibility of process morphology to breakage and deformation. Scanning electron microscopy studies have indeed revealed conical process bases in *S. scottica* and *S. ornata*, which have tentatively been interpreted as resulting from the secondary

collapse of the vesicle wall (Moczydłowska 2011). This likely explains the wide morphological range of specimens attributed to *S. compressa* and *S. ciliosa*, in which the diagnostically conical process bases may derive from the secondary alteration of a variety of *Skiagia* form species. In addition to basal process inflation, the large intraspecific variability of *S. scottica* may also derive from the taphonomic separation and erosion of its process tips, as is suggested by its wide range of P_{ft} and P_E values (Fig. 6D,H) and light microscopic observations (Fig. 9A,C,D).

A key finding of this analysis is that specimens of *S. ciliosa* share a substantial portion of their morphological range with specimens attributed to *S. scottica* (Fig. 8). Although partly attributable to the taphonomic processes highlighted above, the conspicuous overlaps between these two species echo a long-recognized similarity in gross morphology (Knoll and Swett 1987; Young et al. 1994: fig. 10m). The interspecific morphological variance between *S. ciliosa* and *S. scottica* appears to be of a similar magnitude to the intraspecific variability seen within the *S. ciliosa* taxon itself (Downie 1982; Fig. 8). Three different morphotypes of *S. ciliosa* have been previously defined based on process length and width, which show continuous variation (Hagenfeldt 1989; Moczydłowska 1991). The basal process plug seems to be the only feature uniting these morphotypes to *S. ciliosa*, yet similar structures are known from *S. compressa* (Downie 1982; Talyzina and Moczydłowska 2000; Moczydłowska 2011), *S. ornata* (Moczydłowska and Vidal 1986: fig. 11C,D; Hagenfeldt 1989), *S. orbiculare* (Zang 2001; Brück and Vanguestaine 2004), and *S. scottica* (Downie 1982; Zang 2001). At the conventional resolution of light microscopy, identification of a separation between processes and the central body is particularly challenging among acritarchs that possess thin, short, and/or numerous processes with a thick-walled central body (e.g., in *S. ciliosa* morphotype A; Fig. 9F–H). In the studied population, plug-like structures have been observed sporadically in a least four different species, namely *S. scottica* (Fig. 10D,F), *S. ciliosa* (Figs. 2C, 9I, 10G), *S. compressa* (Figs. 2E,G, and 9S) and *S. ornata* (Fig. 2F). The absence of reliable systematic criteria to define the *S. ciliosa* taxon and its morphotypes stands in sharp contrast with the ease of identification that is expected from an index fossil, a property that has frequently been attributed to *S. ciliosa* (Moczydłowska and Zang 2006; Palacios et al. 2020). The morphometric approach adopted here demonstrates that, in a population where the taxonomic significance of basal process plugs appears to be limited, specimens with short processes clearly expanded at the base tend to be more convincingly distinguished from the morphological range of *S. scottica* and *S. orbiculare* (Figs. 8, 9H). However, the taxonomic and biostratigraphic significance of this region of the morphospace remains to be formally assessed through a detailed account of disparity among *Skiagia* populations from successive biozones.

The morphological continuum identified in this study is bounded by our narrow sampling window but can be extended to other acritarch species and genera. For instance, the very slightly flaring process tips of *Skiagia brevispinosa* Downie, 1982 may in fact constitute a transitional form uniting *Skiagia* with other acritarchs such as *Baltisphaeridium cerinum*, which features in the *S. ciliosa* synonymy list (Moczydłowska 1991). Breakage of *Skiagia* processes at their tips results in conspicuous *Baltisphaeridium* morphologies (Zang et al. 2007: fig. 14A–E), while truncation at the base may result in vesicles adorned with thick cones resembling the solid processes of *Globosphaeridium cerinum* (Moczydłowska and Vidal 1986: fig. 9C–F; Vidal and Moczydłowska 1996: fig. 11.4; Yin et al. 2010: fig. 4a,b,g,l; Palacios et al. 2020: fig. 8e–f). At another end of the *Skiagia* morphological spectrum, the extremely regular outline of *S. scottica* occasionally exhibits conspicuous similarities with pteromorph-like acritarchs such as *Fimbriaglomerella* (compare Fig. 10A,F with Moczydłowska and Vidal 1988: figs. 1.5–6). Regardless of their potential origin(s), these striking connections between disparate collections of form taxa tend to suggest that a high level of taxonomic confusion (and potentially inflation) exists beyond that evidenced within the genus *Skiagia* and would warrant a critical evaluation of taxonomic boundaries and co-occurrence patterns using morphometric

means (e.g., Stricanne and Servais 2002; Wang et al. 2017; Yan et al. 2017; Kroeck et al. 2020).

Reconstructing the Life Cycle of *Skiagia*-plexus Acritarchs

The consistency of the *Skiagia* morphotype sequence identified in this study using either morphological (Fig. 8, Supplementary Figs. 4, 6) or ontogenetic parameters (Fig. 11) demonstrates that the species-level classification of *Skiagia* does capture certain elements of phytoplankton paleobiology. Acritarchs have previously been compared to modern phytoplanktonic analogues, including dinoflagellates (e.g., Colbath and Grenfell 1995; Talyzina et al. 2000; Servais et al. 2003, 2004, 2008; Vecoli and Le Hérissé 2004) and green algae (e.g., Colbath and Grenfell 1995; Kaźmierczak and Kremer 2009; Moczydłowska 2010, 2016; Moczydłowska et al. 2011; Agić et al. 2015; Shang et al. 2020). In particular, Moczydłowska (2010) interpreted the continuous morphological range of the *Skiagia* acritarch plexus as representing various encysted stages of the life cycle of one or several species of chlorophycean microalgae. In this model, the first stage, fully planktonic, consists of a vegetative cell that may be represented in the fossil record by a simple sphearomorph (e.g., *Leiosphaeridia*). In a second stage, a cyst is formed within the mother cell or zygote by shrinkage of the cytoplasm, resulting in a morphology reminiscent of *S. scottica*. The vegetative cell and its internal cyst remain in the water column until maturation. At this stage, the outer cell membrane is lost to release the cyst, which sinks to bottom sediments, develops an endocyst, and enters a period of dormancy. This third stage is represented in the fossil record by occurrences of *S. ornata* enclosing a dark internal body (e.g., Moczydłowska 2002: fig. 8.1; Zang et al. 2007: fig. 12A,D). The endocyst is then released into the water column after rupture of the cyst in a fourth stage, to later produce multiple offspring (swarmers) or a single cell that later grows into a new vegetative adult.

Although outer membranes are so far unknown from the taxon *S. scottica*, it has previously been suggested that the wide and flat process tips of this taxon used to be attached to a fragile vegetative cell (Moczydłowska 2010). Close inspection of the exquisitely preserved *S. scottica* population studied here has revealed areas of light-colored, structureless organic material surrounding the processes (Fig. 10A), a potential residual product of a degraded labile outer envelope. Interestingly, similar structures have been observed among transitional forms from *S. scottica* to *S. ciliosa* showing unequal processes (Fig. 10B,C). Although these observations tend to confirm the tight relationships between these species and their immature development, both form taxa exhibit unambiguous excystment structures (Fig. 10E–I), while *S. ciliosa* occasionally develops an endocyst (Volkova 1969; Downie 1982; Palacios et al. 2020; Fig. 11, Supplementary Table 2). The presence of multiple stages in the population of each *Skiagia* species and their relative frequency distribution evidences a complex relationship between them which can hardly be accommodated in a single, regular life cycle.

Most notably, the studied *S. ornata*/*S. compressa* population appears to stand out from other species in terms of excystment rates, endocyst development, and overall morphology (Figs. 4, 8, 11, Table 1), which suggests it captures a distinct type of life cycle, possibly from a distinct biological taxon. In particular, *S. compressa* was the only species yielding a robust population of endocysts, a feature only rarely observed among *Skiagia* (e.g., Moczydłowska et al. 2001; Moczydłowska 2002, 2010; Zang et al. 2007; Palacios et al. 2017, 2020; Supplementary Table 2). It seems, therefore, that endocyst formation is not an obligate stage in the life cycle of *Skiagia*-plexus acritarchs and may instead record occasional environmentally driven alterations of a more conventional life cycle, in which the addition of a second encystment stage ensures an enhanced protection of offspring cells until the return of more favorable conditions. It is also tempting to recognize the recorded variation in the opacity of the internal body as various degrees of endocyst maturation, being most advanced in cysts having undergone longer resting periods. Analogies with modern dinoflagellates indeed suggest that the degree of maturation attained at the end of the period

of dormancy correlates with process length and morphology (Kokinos and Anderson 1995; Servais et al. 2004). This may provide a reliable explanation for the morphological and ontogenetic gradient studied here, culminating in large, encysted vesicles adorned with long processes showing moderately widened bases (Figs. 6, 8, 9). In spite of their apparently mature morphologies, *S. ornata* and *S. compressa* were found to be relatively rarely opened in the studied assemblages (Fig. 11). Failure to release offspring cells after reaching maturity is once again consistent with the interpretation of endocysts as forming a circumstantial ontogenetic stage induced by unusually long periods of environmental stress (e.g., episodes of anoxia, nutrient starvation, or light or temperature stress). As seen in modern dinoflagellate populations (e.g., Rengefors and Anderson 1998; Kremp and Anderson 2000; Bravo and Figueroa 2014), such conditions would force cysts to undergo longer periods of growth in the benthic environment, eventually prohibiting their germination. In this respect, the appearance of endocysts in *Skiagia* assemblages from the *Heliosphaeridium dissimilare–Skiagia ciliosa* Zone (Palacios et al. 2020) may be regarded as a biostratigraphically significant event toward the evolution of complex phytoplanktonic reproduction strategies, demonstrating an advanced mechanism of phenotypic and developmental adaptation to protracted adverse conditions.

It should be stressed that the recorded disparity of *Skiagia* form species and their respective encystment and excystment structures is compatible with the presence of one or several biological species in the studied assemblage. The complexity of phytoplankton lifestyles and their susceptibility to environmental and ecological factors (Sandgren 1983; Anderson et al. 1984; Kokinos and Anderson 1995; Rengefors et al. 1998; Luo et al. 2005; Thornber 2006; Figueroa et al. 2008) implies that morphology-based taxonomic classification systems do not provide a satisfactory delimitation of biological species (e.g., Bold 1974; Kokinos and Anderson 1995). Although our narrow sampling window offers the prospect of clarifying multiple sources of morphological variation, the limitations of applying these quantitative approaches to uncover true taxonomic diversity should be acknowledged.

Refining Our Understanding of Acritarch Diversity

Despite the uncertain affinity of acritarchs and their informal classification scheme, acritarch taxonomic counts have previously been used as a measure of species richness to construct phytoplankton diversity curves at various spatial and temporal scales (Tappan and Loeblich 1973; Vidal and Knoll 1982; Knoll 1994; Strother 1996, 2008; Vidal and Moczydłowska-Vidal 1997; Moczydłowska 1998, 2011; Vecoli and Le Hérissé 2004; Knoll et al. 2006; Li et al. 2007; Mullins and Servais 2008; Klug et al. 2010; Lei et al. 2013; Cohen and Macdonald 2015; Nowak et al. 2015; Riedman and Sadler 2018; Zheng et al. 2020). As the limitations of acritarch form taxonomy have widely been acknowledged, these curves have traditionally been regarded as preservable portions of morphological diversity (i.e., disparity; e.g., Knoll 1994; Cohen and Macdonald 2015) or coarse estimates of true taxonomic diversity (e.g., Vidal and Moczydłowska-Vidal 1997; Zheng et al. 2020). The continuous sequence of *Skiagia* species studied here describes a substantial portion of the total variance (Fig. 4) which, at best, suggests that form-taxonomic counts offer an arbitrary measure of disparity worth five units in the current setting. However, the likelihood of taxonomic confusion resulting from the lack of clear boundaries between form species and genera (e.g., *Baltisphaeridium*) imposes a relatively high degree of uncertainty to this metric. It seems, therefore, that the form-taxonomic subdivision of *Skiagia*-plexus acritarchs currently fails to provide an accurate measure of intrageneric disparity, let alone diversity. Cases of taxonomic inconsistencies and transitional forms in other acritarch genera (e.g., Stricanne and Servais 2002; Vanguestaine 2002; Servais et al. 2004; Kroeck et al. 2021) further question the reliability of form-taxonomic counts as proxies for standing diversity (either morphological or taxonomic).

Whether these form-taxonomic diversity metrics are able to capture significant paleobiological trends beyond additional taphonomic and sampling biases remains to be determined.

Phytoplankton and metazoan diversity curves occasionally show some parallel trends in the Cambrian (Nowak et al. 2015; Zheng et al. 2020), but the exact nature of these isolated correspondences is obscured by the fundamental difference between metazoan and phytoplankton diversity units. Indeed, because the definition of acritarch morphospecies lacks a phylogenetic or paleobiological basis, acritarch diversity does not approximate standing diversity in the manner that natural metazoan groupings do (Butterfield 2004). Any correlation between the metazoan and phytoplankton diversity records should therefore be interpreted with caution. For instance, the sharp rise of acritarch diversity marking the early Cambrian (Vidal and Nystuen 1990; Moczydłowska 2002, 2011; Nowak et al. 2015; Zheng et al. 2020) may be partly attributable to a net increase in the number of biological species, but also to the emergence of more complex heteromorphic life cycles (e.g., Thornber 2006) and an increased likelihood of taxonomic splitting across portions of developmental sequences. Although acritarch diversity curves indirectly capture true, evolutionarily significant events (Cambrian radiation of eukaryotic phytoplankton, alternation of generations in life cycles, developmental adaptability, etc.), form-taxonomic counts and their systematic biases do not offer straightforward pathways to uncover biological diversity, nor do they provide accurate measures of evolutionary tempo.

The problems surrounding these taxonomic counts have triggered a search for alternative measures of diversity, with an increased focus on key characters elucidating cell function and development (Huntley et al. 2006; Knoll et al. 2006; Moczydłowska 2011; Cohen and Macdonald 2015). Even so, these elements of phytoplankton paleobiology have often been highlighted (Moczydłowska 2011) or coarsely quantified (Knoll et al. 2006; Cohen and Mcdonald 2015) on top of conventional form-species richness and its inevitable reliance on arbitrary taxonomic practices. The morphometric approach developed by Huntley et al. (2006) is unique in that it proposes disparity measures that are fully independent from taxonomic subdivisions or presumed phylogenetic affinities, being defined based on a universal presence–absence character matrix. An inevitable caveat of these methods is their dependence on the choice of characters used for dissimilarity and variance calculations, each trait being given equal weight regardless of its paleobiological significance. The results of this study show that, in addition to discrete features (e.g., endocysts and excystment structures), acritarch vesicles exhibit continuous morphological variations that may result from a complex life cycle and/or record adaptations to local environmental or paleoecological conditions. Application of similar morphometric techniques to specimens from elsewhere may help clarify the patterns of disparity exhibited by acritarch taxa within and beyond the genus *Skiagia*, revealing the key morphological traits that underpin them, and perhaps providing clues on their affinities and adaptive significance.

Conclusions

The uncertain and polyphyletic nature of Cambrian acritarchs constitutes a persistent obstacle to establishing consistent classification systems. Here we used a quantitative approach to clarify the morphological basis of the species-level taxonomy of acritarchs from the genus *Skiagia* and assessed its paleobiological significance. The following key findings have been brought to light:

- The species-level classification of *Skiagia* acritarchs discretizes a continuous suite of morphologies.
- The arbitrariness of species boundaries is a source of taxonomic and biostratigraphic confusion.
- The species-level classification of *Skiagia* acritarchs does reflect certain elements of phytoplankton paleobiology, including the relative contribution of ontogenetic, paleoenvironmental, and paleoecological factors on process morphology.
- *Skiagia* form-taxonomic counts do not provide unequivocal measures of true diversity or disparity.

Similar morphometric analyses of acritarch populations worldwide hold great promise to clarify the multivariate disparity of acritarch

form taxa and refine their boundaries based on consistent patterns of stratigraphic and/or paleoenvironmental variation. Continued exploration of phenotypic plasticity among Cambrian acritarchs would greatly refine our understanding of these problematic fossils, and by extension our knowledge of the earliest Phanerozoic-style primary producers.

Acknowledgments

M. Moczydłowska-Vidal and J. S. Peel are thanked for guidance and help in interpreting the material and the geology. Samples were collected during fieldwork supported by the Geological Survey of Greenland. B.J.S. acknowledges the support of Swedish Research Council (VR) grant 2020-03314. H. Agić, J. W. Huntley, and an anonymous reviewer are thanked for their constructive feedback on a previous version of this paper.

Data Availability Statement

Data available from the Dryad Digital Repository: https://doi.org/10.5061/dryad.zs7h44jbv.

Literature Cited

Agić, H., M. Moczydłowska, and L.-M. Yin. 2015. Affinity, life cycle, and intracellular complexity of organic-walled microfossils from the Mesoproterozoic of Shanxi, China. Journal of Paleontology 89:28–50.

Ahn, S. Y., and M. Zhu. 2017. Lowermost Cambrian acritarchs from the Yanjiahe Formation, South China: implication for defining the base of the Cambrian in the Yangtze Platform. Geological Magazine 154:1217–1231.

Albrecht, G. H. 1980. Multivariate analysis and the study of form, with special reference to canonical variate analysis. American Zoologist 20:679–693.

Álvarez, S. G., C. M. Juaristi, J. S. Gutierrez, and I. García-Amorena. 2009. Taxonomic differences between *Pinus sylvestris* and *P. uncinata* revealed in the stomata and cuticle characters for use in the study of fossil material. Review of Palaeobotany and Palynology 155:61–68.

Anderson, D. M., D. M. Kulis, and B. J. Binder. 1984. Sexuality and cyst formation in the dinoflagellate *Gonyaulax tamarensis*: cyst yield in batch cultures. Journal of Phycology 20:418–425.

Anderson, M. J. 2017. Permutational multivariate analysis of variance (PERMANOVA). Wiley StatsRef: Statistics Reference Online. doi: 10.1002/9781118445112.stat07841.

Bold, H. C. 1974. Phycology, 1947–1972. Annals of the Missouri Botanical Garden 61:14–44.

Bravo, I., and R. I. Figueroa. 2014. Towards an ecological understanding of dinoflagellate cyst functions. Microorganisms 2:11–32.

Brück, P. M., and M. Vanguestaine. 2004. Acritarchs from the Lower Palaeozoic succession on the south County Wexford coast, Ireland: new age constraints for the Cullenstown Formation and the Cahore and Ribband Groups. Geological Journal 39:199–224.

Butterfield, N. J. 1997. Plankton ecology and the Proterozoic–Phanerozoic transition. Paleobiology 3:247–262.

Butterfield, N. J. 2004. A vaucheriacean alga from the middle Neoproterozoic of Spitsbergen: implications for the evolution of Proterozoic eukaryotes and the Cambrian explosion. Paleobiology 30:231–252.

Butterfield, N. J. 2005a. Probable proterozoic fungi. Paleobiology 31:165–182.

Butterfield, N. J. 2005b. Reconstructing a complex early Neoproterozoic eukaryote, Wynniatt Formation, arctic Canada. Lethaia 38:155–169.

Butterfield, N. J. 2007. Macroevolution and macroecology through deep time. Palaeontology 50:41–55.

Butterfield, N. J. 2011. Animals and the invention of the Phanerozoic Earth system. Trends in Ecology and Evolution 26:81–87.

Butterfield, N. J., A. H. Knoll, and K. Swett. 1994. Paleobiology of the Neoproterozoic Svanbergfjellet Formation, Spitsbergen. Fossils and Strata 34:1–84.

Campbell, N. A., and W. R. Atchley. 1981. The geometry of canonical variate analysis. Systematic Biology 30:268–180.

Carranza, N. L., and S. J. Carlson. 2021. Quantifying shell outline variability in extant and fossil *Laqueus* (Brachiopoda: Terebratulida): are outlines good proxies for long-looped brachidial morphology and can they help us characterize species? Paleobiology 47:149–170.

Cheetham, A. H. 1986. Tempo of evolution in a Neogene bryozoan: rates of morphologic change within and across species boundaries. Paleobiology 12:190–202.

Cohen, P. A., and F. A. Macdonald. 2015. The Proterozoic record of eukaryotes. Paleobiology 41:610–632.

Colbath, G. K., and H. R. Grenfell. 1995. Review of biological affinities of Paleozoic acid-resistant, organic-walled eukaryotic algal microfossils (including "acritarchs"). Review of Palaeobotany and Palynology 86:287–314.

De Meulemeester, T., D. Michez, A. M. Aytekin, and B. N. Danforth. 2012. Taxonomic affinity of halictid bee fossils (Hymenoptera: Anthophila) based on geometric morphometrics analyses of wing shape. Journal of Systematic Palaeontology 10:755–764.

Downie, C. 1982. Lower Cambrian acritarchs from Scotland, Norway, Greenland and Canada. Transactions of the Royal Society of Edinburgh (Earth and Environmental Sciences) 72:257–285.

Downie, C., W. R. Evitt, and W. A. S. Sarjeant. 1963. Dinoflagellates, hystrichospheres, and the classification of the acritarchs. Stanford University Publications, Geological Sciences 7:1–16.

Ellegaard, M. 2000. Variations in dinoflagellate cyst morphology under conditions of changing salinity during the last 2000 years in the Limfjord, Denmark. Review of Palaeobotany and Palynology 109:65–81.

Evitt, W. R. 1963. A discussion and proposals concerning fossil dinoflagellates, hystrichospheres, and acritarchs, II. Proceedings of the National Academy of Sciences USA 49:298–302.

Fatka, O., and R. Brocke. 2008. Morphologic variability in lower Palaeozoic acritarchs: importance for acritarch systematics. Acta Musei Nationalis Pragae, series B, Historia Naturalis 64:97–107.

Figueroa, R. I., I. Bravo, and E. Garcés. 2008. The significance of sexual versus asexual cyst formation in the life cycle of the noxious dinoflagellate *Alexandrium peruvianum*. Harmful Algae 7:653–663.

Geary, D. H. 1992. An unusual pattern of divergence between two fossil gastropods: ecophenotypy, dimorphism, or hybridization? Paleobiology 18:93–109.

Grey, K., and S. Willman. 2009. Taphonomy of Ediacaran acritarchs from Australia: significance for taxonomy and biostratigraphy. Palaios 24:239–256.

Hagenfeldt, S. E. 1989. Lower Cambrian acritarchs from the Baltic Depression and south-central Sweden, taxonomy and biostratigraphy. Stockholm Contributions in Geology 41:1–176.

Hammer, Ø., and D. A. T. Harper. 2006. Paleontological data analysis. Blackwell, Oxford, U.K.

Hammer, Ø., D. A. T. Harper, and P. D. Ryan. 2001. PAST: paleontological statistics software package for education and data analysis. Palaeontologia Electronica 4:1–9.

Higgins, A. K., J. R. Ineson, J. S. Peel, F. Surlyk, and M. Sønderholm. 1991. Lower Palaeozoic Franklinian basin of North Greenland. Bulletin Grønlands Geologiske Undersøgelse 160:71–139.

Hollingsworth, J. S. 2011. Lithostratigraphy and biostratigraphy of Cambrian Stage 3 in western Nevada and eastern California. Museum of Northern Arizona Bulletin 67:26–42.

Huntley, J. W. 2011. Exploratory multivariate techniques and their utility for understanding ancient ecosystems. Pp. 23–48 *in* M. Laflamme, J. D. Schiffbauer, and S. Q. Dornbos, eds. Quantifying the evolution of early life: numerical approaches to the evaluation of fossils and ancient ecosystems. Springer, Dordrecht, Netherlands.

Huntley, J. W., S. Xiao, and M. Kowalewski. 2006. 1.3 billion years of acritarch history: an empirical morphospace approach. Precambrian Research 144:52–68.

Ineson, J. R., and J. S. Peel. 1997. Cambrian shelf stratigraphy of North Greenland. Geology of Greenland Survey Bulletin 173:1–120.

Ineson, J. R., and J. S. Peel. 2011. Geological and depositional setting of the Sirius Passet *Lagerstätte* (Early Cambrian), North Greenland. Canadian Journal of Earth Sciences 48:1259–1281.

Jankauskas, T.V. 1976. Novyje vidy akritarkh iz nizhnego kembrija Pribaltiki (New acritarch species from the Lower Cambrian in the Baltic republics). Pp. 187–194 *in* I. T. Zhuravleva, ed. Stratigraflya i paleontologiya nizhnego i srednego kembriya SSSR (Stratigraphy and palaeontology of the Lower and Middle Cambrian in the USSR). Nauka, Novosibirsk.

Javaux, E. J., and A. H. Knoll. 2017. Micropaleontology of the lower Mesoproterozoic Roper Group, Australia, and implications for early eukaryotic evolution. Journal of Paleontology 91:199–229.

Kaźmierczak, J., and B. Kremer. 2009. Spore-like bodies in some early Paleozoic acritarchs: clues to chlorococcalean affinities. Acta Palaeontologica Polonica 54:541–551.

Kirjanov, V.V. 1974. Novye akritarkhi iz kembrijskikh otlozhenij Volyni (New acritarchs from the Cambrian deposits of Volhynia). Paleontologicheskii Zhurnal 2:117–130.

Klug, C., B. Kröger, W. Kiessling, G. L. Mullins, T. Servais, J. Frýda, D. Korn, and S. Turner. 2010. The Devonian nekton revolution. Lethaia 43:465–477.

Knoll, A. H. 1994. Proterozoic and early Cambrian protists: evidence for accelerating evolutionary tempo. Proceedings of the National Academy of Sciences USA 91:6743–6750.

Knoll, A. H., and K. Swett. 1987. Micropaleontology across the Precambrian–Cambrian boundary in Spitsbergen. Journal of Paleontology 61:898–926.

Knoll, A. H., E. J. Javaux, D. Hewitt, and P. Cohen. 2006. Eukaryotic organisms in Proterozoic oceans. Philosophical Transactions of the Royal Society of London B 361:1023–1038.

Kokinos, J. P., and D. M. Anderson. 1995. Morphological development of resting cysts in cultures of the marine dinoflagellate *Lingulodinium polyedrum* (= *L.* machaerophorum*). Palynology* 19:143–166.

Kowalewski, M., E. Dyreson, J. D. Marcot, J. A. Vargas, K. W. Flessa, and D. P. Hallman. 1997. Phenetic discrimination of biometric simpletons: paleobiological implications of morphospecies in the lingulide brachiopod *Glottidia*. Paleobiology 23:444–469.

Kremp, A., and D. M. Anderson. 2000. Factors regulating germination of resting cysts of the spring bloom dinoflagellate *Scrippsiella hangoei* from the northern Baltic Sea. Journal of Plankton Research 22:1311–1327.

Kroeck, D. M., M. Blanchon, A. Zacaï, N. Navidi-Izad, H. B. Benachour, C. Monnet, E. Raevskaya, Z. Szczepanik, and T. Servais. 2020. Revision of the Cambro-Ordovician acritarch genus *Vulcanisphaera* Deunff, 1961. Review of Palaeobotany and Palynology 279:104212.

Kroeck, D. M., M. E. Eriksson, A. Lindskog, A. Munnecke, M. Dubois, S. Régnier, and T. Servais. 2021. Morphological variability of peteinoid acritarchs from the Middle Ordovician of Öland, Sweden, and implications for acritarch classification. Palynology 45:705–715.

Labandeira, C. C., and N. C. Hughes. 1994. Biometry of the Late Cambrian trilobite genus *Dikelocephalus* and its implications for trilobite systematics. Journal of Paleontology 68:492–517.

Lance, R. F., M. L. Kennedy, and P. L. Leberg. 2000. Classification bias in discriminant function analyses used to evaluate putatively different taxa. Journal of Mammalogy 81:245–249.

Landing, E., G. Geyer, M. D. Brasier, and S. A. Bowring. 2013. Cambrian evolutionary radiation: context, correlation, and chronostratigraphy—overcoming deficiencies of the first appearance datum (FAD) concept. Earth-Science Reviews 123:133–172.

Le Hérissé, A. 1989. Acritarches et kystes d'algues prasinophycées du Silurien de Gotland, Suède. Palaeontographia Italica 76:57–302.

Lei, Y., T. Servais, and Q. Feng. 2013. The diversity of the Permian phytoplankton. Review of Palaeobotany and Palynology 198:145–161.

Li, J., T. Servais, K. Yan, and W. Su. 2007. Microphytoplankton diversity curves of the Chinese Ordovician. Bulletin de la Société Géologique de France 178:399–409.

Lohmann, G. P. 1983. Eigenshape analysis of microfossils: a general morphometric procedure for describing changes in shape. Journal of the International Association for Mathematical Geology 15:659–672.

Luo, W., L. Krienitz, S. Pflugmacher, and N. Walz. 2005. Genus and species concept in *Chlorella* and *Micractinium* (Chlorophyta, Chlorellaceae): genotype versus phenotypical variability under ecosystem conditions. Internationale Vereinigung für theoretische und angewandte Limnologie: Verhandlungen 29:170–173.

Marko, P. B., and J. B. Jackson. 2001. Patterns of morphological diversity among and within arcid bivalve species pairs separated by the Isthmus of Panama. Journal of Paleontology 75:590–606.

Marramà, G., and J. Kriwet. 2017. Principal component and discriminant analyses as powerful tools to support taxonomic identification and their use for functional and phylogenetic signal detection of isolated fossil shark teeth. PLoS ONE 12:e0188806.

McLachlan, G. J. 1999. Mahalanobis distance. Resonance 4:20–26.

Moczydłowska, M. 1988. New Lower Cambrian acritarchs from Poland. Review of Palaeobotany and Palynology 54:1–10.

Moczydłowska, M. 1991. Acritarch biostratigraphy of the Lower Cambrian and the Precambrian–Cambrian boundary in southeastern Poland. Fossils and Strata 29:1–127.

Moczydłowska, M. 1998. Cambrian acritarchs from Upper Silesia, Poland—biochronology and tectonic implications. Fossils and Strata 46:1–121.

Moczydłowska, M. 1999. The Lower-Middle Cambrian boundary recognised by acritarchs in Baltica and at the margin of Gondwana. Bolletino della Societa Paleonologica Italiana 38:207–225.

Moczydłowska, M. 2002. Early Cambrian phytoplankton diversification and appearance of trilobites in the Swedish Caledonides with implications for coupled evolutionary events between primary producers and consumers. Lethaia 35:191–214.

Moczydłowska, M. 2010. Life cycle of early Cambrian microalgae from the *Skiagia*-plexus acritarchs. Journal of Paleontology 84:216–230.

Moczydłowska, M. 2011. The early Cambrian phytoplankton radiation: acritarch evidence from the Lükati Formation, Estonia. Palynology 35:103–145.

Moczydłowska, M. 2016. Algal affinities of Ediacaran and Cambrian organic-walled microfossils with internal reproductive bodies: *Tanarium* and other morphotypes. Palynology 40:83–121.

Moczydłowska, M., and G. Vidal. 1986. Lower Cambrian acritarch zonation in southern Scandinavia and southeastern Poland. Geologiska Föreningen i Stockholm Förhandlingar 108:201–223.

Moczydłowska, M., and G. Vidal. 1988. Early Cambrian acritarchs from Scandinavia and Poland. Palynology 12:1–10.

Moczydłowska, M., and S. Willman. 2009. Ultrastructure of cell walls in ancient microfossils as a proxy to their biological affinities. Precambrian Research 173:27–38.

Moczydłowska, M., and W. L. Zang. 2006. The Early Cambrian acritarch *Skiagia* and its significance for global correlation. Palaeoworld 15:328–347.

Moczydłowska, M., S. Jensen, J. O. R. Ebbestad, G. E. Budd, and M. Marti-Mus. 2001. Biochronology of the autochthonous Lower Cambrian in the Laisvall–Storuman area, Swedish Caledonides. Geological Magazine 138:435–453.

Moczydłowska, M., E. Landing, W. Zang, and T. Palacios. 2011. Proterozoic phytoplankton and timing of Chlorophyte algae origins. Palaeontology 54:721–733.

Molyneux, S. G., A. Delabroye, R. Wicander, and T. Servais. 2013. Biogeography of early to mid Palaeozoic (Cambrian–Devonian) marine phytoplankton. Geological Society of London Memoir 38:365–397.

Mullins, G. L., and T. Servais. 2008. The diversity of the Carboniferous phytoplankton. Review of Palaeobotany and Palynology 149:29–49.

Naselli-Flores, L., J. Padisák, and M. Albay. 2007. Shape and size in phytoplankton ecology: do they matter? Hydrobiologia 578:157–161.

Naumova, S.N. 1960. Sporogo-pyltsevye kompleksy rifejskikh i nizhnekembrijskikh otlozhenij SSSR (Spore-pollen assemblages of the Riphean and Lower Cambrian deposits in the USSR). Pp. 109–117 *in* Stratigrafiya pozdnego dokembriya i kembriya. Mezhdynarodnyj geolagicheskij kongres 21 sessii. Doklady sovetskikh geologov (Stratigraphy of the late Precambrian and Cambrian. International Geological Congress 21 session. Reports of the Soviet geologists). Akademia Nauk SSSR, Moscow.

Nowak, H., T. Servais, C. Monnet, S. G. Molyneux, and T. R. A. Vandenbroucke. 2015. Phytoplankton dynamics from the Cambrian Explosion to the onset of the Great Ordovician Biodiversification Event: a review of Cambrian acritarch diversity. Earth-Science Reviews 151:117–131.

Palacios, T., and M. Moczydłowska. 1998. Acritarch biostratigraphy of the Lower-Middle Cambrian boundary in the Iberian Chains, province of Soria, northeastern Spain. Revista Española de Paleontología, Numero Extraordinario 13:65–82.

Palacios, T., S. Jensen, S. M. Barr, C. E. White, and R. F. Miller. 2011. New biostratigraphical constraints on the lower Cambrian Ratcliffe Brook Formation, southern New Brunswick, Canada, from organic-walled microfossils. Stratigraphy 8:45–60.

Palacios, T., S. Jensen, S. M. Barr, C. E. White, and R. F. Miller. 2017. Acritarchs from the Hanford Brook Formation, New Brunswick, Canada: new biochronological constraints on the *Protolenus elegans* Zone and the Cambrian Series 2–3 transition. Geological Magazine 154:571–590.

Palacios, T., S. Jensen, S. M. Barr, C. E. White, and P. M. Myrow. 2018. Organic-walled microfossils from the Ediacaran–Cambrian boundary stratotype section, Chapel Island and Random formations, Burin Peninsula, Newfoundland, Canada: global correlation and significance for the evolution of early complex ecosystems. Geological Journal 53:1728–1742.

Palacios, T., A. E. S. Högström, J. O. R. Ebbestad, H. Agić, M. Høyberget, S. Jensen, G. Meinhold, and W. L. Taylor. 2020. Acritarchs from the Duolbagáisá Formation (Cambrian Series 2, Miaolingian) on the Digermulen Peninsula, Finnmark, Arctic Norway: towards a high-resolution Cambrian chronostratigraphy. Geological Magazine 157:2051–2066.

Peel, J. S., and S. Willman. 2018. The Buen Formation (Cambrian Series 2) biota of North Greenland. Papers in Palaeontology 4:381–432.

Peterson, K. J., and N. J. Butterfield. 2005. Origin of the Eumetazoa: testing ecological predictions of molecular clocks against the Proterozoic fossil record. Proceedings of the National Academy of Sciences USA 102:9547–9552.

Reichenbacher, B., U. Sienknecht, H. Küchenhoff, and N. Fenske. 2007. Combined otolith morphology and morphometry for assessing taxonomy and diversity in fossil and extant killifish (Aphanius, †Prolebias). Journal of Morphology 268:898–915.

Rengefors, K., and D. M. Anderson. 1998. Environmental and endogenous regulation of cyst germination in two freshwater dinoflagellates. Journal of Phycology 34:568–577.

Rengefors, K., I. Karlsson, and L. Hansson. 1998. Algal cyst dormancy: a temporal escape from herbivory. Proceedings of the Royal Society of London B 265:1353–1358.

Reyment, R. A. 2003. Morphometric analysis of variability in the shell of some Nigerian Turonian (Cretaceous) ammonites. Cretaceous Research 24:789–803.

Riedman, L. A., and P. M. Sadler. 2018. Global species richness record and biostratigraphic potential of early to middle Neoproterozoic eukaryote fossils. Precambrian Research 319:6–18.

Rueden, C. T., J. Schindelin, M. C. Hiner, B. E. DeZonia, A. E. Walter, E. T. Arena, and K. W. Eliceiri. 2017. ImageJ2: ImageJ for the next generation of scientific image data. BMC Bioinformatics 18:1–26.

Rushton, A. W. A., P. M. Brück, S. G. Molyneux, M. Williams, and N. H. Woodcock. 2011. A revised correlation of the Cambrian rocks in the British Isles, Vol. 25. Geological Society of London, London.

Sandgren, C. D. 1983. Morphological variability in populations of Chrysophycean resting cysts. I. Genetic (interclonal) and encystment temperature effects on morphology. Journal of Phycology 19:64–70.

Schneider, C. A., W. S. Rasband, and K. W. Eliceiri. 2012. NIH Image to ImageJ: 25 years of image analysis. Nature Methods 9:671–675.

Servais, T., J. Li, S. Molyneux, and E. Raevskaya. 2003. Ordovician organic-walled microphytoplankton (acritarch) distribution: the global scenario. Palaeogeography, Palaeoclimatology, Palaeoecology 195:149–172.

Servais, T., L. Stricanne, M. Montenari, and J. Pross. 2004. Population dynamics of galeate acritarchs at the Cambrian–Ordovician transition in the Algerian Sahara. Palaeontology 47:395–414.

Servais, T., O. Lehnert, J. U. N. Li, G. L. Mullins, A. Munnecke, A. Nuetzel, and M. Vecoli. 2008. The Ordovician Biodiversification: revolution in the oceanic trophic chain. Lethaia 41:99–109.

Shang, X., P. Liu, M. Moczydłowska, and B. Yang. 2020. Algal affinity and possible life cycle of the early Cambrian acritarch *Yurtusia uniformis* from South China. Palaeontology 63:903–917.

Sheets, H. D., K. Kim, and C. E. Mitchell. 2004. A combined landmark and outline-based approach to ontogenetic shape change in the Ordovician trilobite *Triarthrus becki*. Pp. 67–82 *in* A. M. T. Elewa, ed. Morphometrics: applications in biology and paleontology. Springer, Berlin.

Slater, B. J., and G. E. Budd. 2019. Comment on: Tang et al. [2019]: A problematic animal fossil from the early Cambrian Hetang Formation, South China. Journal of Paleontology 93:1276–1278.

Slater, B. J., and S. Willman. 2019. Early Cambrian small carbonaceous fossils (SCFs) from an impact crater in western Finland. Lethaia 52:570–582.

Slater, B. J., S. Willman, G. E. Budd, and J. S. Peel. 2018. Widespread preservation of small carbonaceous fossils (SCFs) in the early Cambrian of North Greenland. Geology 46:107–110.

Soper, N. J., and A. K. Higgins. 1987. A shallow detachment beneath the North Greenland fold belt: implications for sedimentation and tectonics. Geological Magazine 124:441–450.

Strauss, R. E. 2010. Discriminating groups of organisms. Pp. 73–91 *in* A. M. T. Elewa, ed. Morphometrics for nonmorphometricians. Springer, Berlin.

Stricanne, L., and T. Servais. 2002. A statistical approach to classification of the Cambro–Ordovician galeate acritarch plexus. Review of Palaeobotany and Palynology 118:239–259.

Strother, P. K. 1996. Acritarchs. Pp. 81–106 *in* J. Jansonius and D. C. McGregor, eds. Palynology: principles and applications. American Association of Stratigraphic Palynologists Foundation, Salt Lake City, Utah.

Strother, P. K. 2008. A speculative review of factors controlling the evolution of phytoplankton during Paleozoic time. Revue de Micropaléontologie 51:9–21.

Talyzina, N. M., and M. Moczydłowska. 2000. Morphological and ultrastructural studies of some acritarchs from the Lower Cambrian Lükati Formation, Estonia. Review of Palaeobotany and Palynology 112:1–21.

Talyzina, N. M., J. M. Moldowan, A. Johannisson, and F. J. Fago. 2000. Affinities of Early Cambrian acritarchs studied by using microscopy, fluorescence flow cytometry and biomarkers. Review of Palaeobotany and Palynology 108:37–53.

Tappan, H. 1980. The paleobiology of plant protists. Freeman, San Francisco.

Tappan, H., and A. R. Loeblich. 1973. Evolution of the oceanic plankton. Earth-Science Reviews 9:207–240.

Thornber, C. S. 2006. Functional properties of the isomorphic biphasic algal life cycle. Integrative and Comparative Biology 46:605–614.

Vanguestaine, M. 2002. The Late Cambrian acritarch *Cristallinium randomense*: morphology, taxonomy and stratigraphical extension. Review of Palaeobotany and Palynology 118:269–285.

Vanguestaine, M., P. M. Brück, N. Maziane-Serraj, and K. T. Higgs. 2002. Cambrian palynology of the Bray Group in County Wicklow and south County Dublin, Ireland. Review of Palaeobotany and Palynology 120:53–72.

Vecoli, M., and A. Le Hérissé. 2004. Biostratigraphy, taxonomic diversity and patterns of morphological evolution of Ordovician acritarchs (organic-walled microphytoplankton) from the northern Gondwana margin in relation to palaeoclimatic and palaeogeographic changes. Earth-Science Reviews 67:267–311.

Vidal, G. 1988. A palynological preparation method. Palynology 12:215–220.

Vidal, G., and A. H. Knoll. 1982. Radiations and extinctions of plankton in the late Proterozoic and early Cambrian. Nature 297:57–60.

Vidal, G., and M. Moczydłowska. 1996. Vendian Lower Cambrian acritarch biostratigraphy of the central Caledonian fold belt in Scandinavia and the palaeogeography of the Iapetus-Tornquist seaway. Norsk Geologisk Tidsskrift 76:147–168.

Vidal, G., and M. Moczydłowska-Vidal. 1997. Biodiversity, speciation, and extinction trends of Proterozoic and Cambrian phytoplankton. Paleobiology 23:230–246.

Vidal, G., and J. P. Nystuen. 1990. Lower Cambrian acritarchs and the Proterozoic Cambrian boundary in southern Norway. Norsk Geologisk Tidsskrift 70:191–222.

Vidal, G., and J. S. Peel. 1993. Acritarchs from the Lower Cambrian Buen Formation in North Greenland. Grønlands Geologiske Undersøgelse Bulletin 164:1–35.

Volkova, N. A. 1968. Akritarkhi dokembrijskikh i nizhnekembrijskikh otlozhenij Estonii (Acritarchs from the Precambrian and Cambrian deposits of Estonia). Pp. 8–36 *in* N. A. Volkova, Z. A. Zhuravleva, V. E. Zabrodin, and B. Sh. Klinger, eds. Problematiki Pogranichnykh Sloev Rifeya i Kembriya Russkoj Platformy, Urala i Kazakhstana (Problematics of Riphean and Cambrian Layers of the Russian Platform, Urals and Kazakhstan). Nauka, Moscow.

Volkova, N. A. 1969. Akritarkhi severo-zapada Russkoj platformy (Acritarchs of the north-western Russian platform). Pp. 224–236 *in* A. Yu. Rozanov, V. V. Missarzhevskij, and N. A. Volkova, eds. Tommotskij Yarus i Problema Nizhnej Granitsy Kembriya (Tommotian Stage and the Cambrian Lower Boundary Problem). Nauka, Moscow.

Volkova, N. A., V. V. Kirjanov, L. V. Piscun, L. T. Pashkyavichene, and T. V. Jankauskas. 1979. Rastitelnye mikrofossili. Pp. 4–38 *in* B. M. Keller and A. Yu. Rozanov, eds. Paleontologija verkhnedokembrijskikh i kembrijskikh otlozhenij Vostochno-Evropejskoj platformy (Upper Precambrian and Cambrian palaeontology of the East-European Platform). Nauka, Moscow.

Wallet, E., B. J. Slater, S. Willman, and J. S. Peel. 2021. Small carbonaceous fossils (SCFs) from North Greenland: new light on metazoan diversity in early Cambrian shelf environments. Papers in Palaeontology 7:1403–1433.

Wang, W., C. Monnet, and T. Servais. 2017. Quantitative methods used for understanding the taxonomy of acritarchs: a case study of the Middle Ordovician genus *Frankea* Burmann 1970. Palynology 41:69–79.

Willman, S., and M. Moczydłowska. 2007. Wall ultrastructure of an Ediacaran acritarch from the Officer Basin, Australia. Lethaia 40:111–123.

Yan, K., J. Li, S. G. Molyneux, E. G. Raevskaya, and T. Servais. 2017. A review of the Ordovician acritarch genus *Barakella* Cramer & Díez 1977. Palynology 41:80–94.

Yin, L. M., Y. L. Zhao, R. D. Yang, and J. Peng. 2010. Acritarchs from the early-middle Cambrian Kaili formation in the Wuliu-Zengjiaya section, east Guizhou Province, China. Acta Palaeontologica Sinica 49:164–173.

Young, T., F. Martin, W. T. Dean, and A. W. A. Rushton. 1994. Cambrian stratigraphy of St Tudwal's Peninsula, Gwynedd, northwest Wales. Geological Magazine 131:335–335.

Zang, W.-L. 2001. Acritarchs. Pp. 74–85 *in* E. M. Alexander, J. B. Jago, A. Y. Rozanov, and A. Y. Zhuravlev, eds. The Cambrian biostratigraphy of the Stansbury Basin, South Australia, Vol. 282. Russian Academy of Sciences, Nauka, Moscow.

Zang, W.-L., M. Moczydłowska, and J. B. Jago. 2007. Early Cambrian acritarch assemblage zones in South Australia and global correlation. Memoirs of the Association of Australasian Palaeontologists 33:141–177.

Zhang, X., P. Ahlberg, L. E. Babcock, D. K. Choi, G. Geyer, R. Gozalo, J. Stewart Hollingsworth, G. Li, E. B. Naimark, T. Pegel, M. Steiner, T. Wotte, and Z. Zhang. 2017. Challenges in defining the base of Cambrian Series 2 and Stage 3. Earth-Science Reviews 172:124–139.

Zheng, S., S. Clausen, Q. Feng, and T. Servais. 2020. Review of organic-walled microfossils research from the Cambrian of China: implications for global phytoplankton diversity. Review of Palaeobotany and Palynology 276:104191.